Graduate School of Frontier Biosciences

Osaka University

Neural basis of correct and inverted judgments in a crossed-hands tactile temporal order judgment task

A thesis submitted to the Graduate Office in fulfillment

of requirements for the degree of Doctor of Philosophy

in Neurosciences

Author:

Ali Moharramipour

Supervisor:

Shigeru Kitazawa

January 2022

Summary

If we are asked to judge the temporal order of two successive tactile stimuli delivered to each hand, we often make inverted judgments when we cross our hands. This phenomenon, termed the crossing effect, indicates that our brain utilizes not only the somatosensory information but the posture-related spatial information in the perception of touch and its temporal order. In the present thesis, I examined the neural basis associated with the crossing of the hands and making an inverted judgment.

I first paid attention to the fact that the degree of reversal (i.e., making inverted judgments due to the crossing of the hands) varies significantly across individuals. The brain regions responsible for the inter-individual variability should play a major role in the crossing effect. I then turned to the intra-individual variability. Each individual makes inverted judgments in some of the trials and not the others. To study the trial-by-trial variability, I examined the time-frequency dynamics of the interactions between those regions associated with the crossing effect.

In the first part, by analyzing the structural MRI image of different individuals, I discovered that the participants with a thinner, larger, and more convoluted cerebral cortex in ten anatomical regions, including the right pars-orbitalis, right and left postcentral gyri, left precuneus, left superior parietal lobule, right middle temporal gyrus, left superior temporal gyrus, right cuneus, left supramarginal gyrus, and right rostral middle frontal gyrus had a smaller degree of reversal. I hypothesize that a better cortical elaboration (development) in those ten regions should contribute to better integrating the somatosensory and spatial postural information and a superior top-down inhibitory control.

In the second part, I analyzed magnetoencephalographic data to derive the dynamic network connectivity across the regions found in the first part. I discovered that there were two distinct

modes in the brain network connectivity, one in the low alpha band (5~10 Hz) and the other in the low beta band (12~18 Hz). When the hands were uncrossed, the brain mainly utilized the low alpha mode, and the low alpha connectivity was dominated by one of the hemispheres contralateral to the hand being stimulated first. On the contrary, when the hands were crossed, the low beta mode was profoundly recruited as well, and the connectivity involved both hemispheres. Most importantly, the low beta mode connectivity was less recruited in the trials with inverted judgments and the participants with a larger degree of judgment reversal.

The present study suggests that the brain network involving the ten brain regions is responsible for ordering the tactile signals represented in both somatotopic and spatial coordinates. Furthermore, the network utilizes the low alpha band by default, but the low alpha mode yields inverted judgments when the hands are crossed. The recruitment of the low beta mode is a major contributor to making a correct judgment.

Keywords: tactile temporal order judgment (TOJ), judgment reversal, structural MRI, cortical characteristics, magnetoencephalography, functional connectivity, touch

Table of contents

General Introduction

Our brain can detect the temporal order of two successive tactile stimuli delivered to each hand with a stimulus onset asynchrony (SOA) of as short as 20~50 ms (Hirsh IJ and CE Sherrick Jr 1961; Pöppel E 1997). It is noteworthy that the short SOA of around 50 ms is quite challenging, and we might sometimes fail in successfully identifying the order. However, when the SOA is above 100 ms, it is easy to detect the order, consistently without failure. Interestingly, when we cross our hands, the task difficulty increases drastically to a degree that we often perceive the order inversely even when the SOA is long, around hundreds of milliseconds (Fig. 0-1) (Yamamoto S and S Kitazawa 2001; Shore DI et al. 2002). This phenomenon suggests that our brain doesn't rely solely on its somatotopic arrangement (point-by-point correspondence between body areas and the primary somatosensory cortex) in the perception of the touch and its temporal order but also considers the body posture. As the somatosensory information coming from the somatotopic arrangement is not altered by the crossing of the hands, the integration of the posture-related spatial information with the somatosensory information should be causing the inverted perception.

This phenomenon, known as the crossing effect or the judgment reversal, was discovered by Yamamoto S and S Kitazawa (2001) for the first time in 2001. Since then, it has gotten lots of attention in the scientific community. The crossing effect indicates that the somatosensory and proprioceptive (sense of own body posture) systems should interact for perceiving a touch on the hands. Thus, the study of the crossing effect could reveal the neural basis of those systems and their interactions. It can contribute to discovering how our brain makes an internal map of the body's posture, how it processes and updates this internal map, and how it utilizes this map in the somatosensory system for the perception of touch. Last, it is worth nothing that it can even impact

medical science by better understanding the underlying problem of the patients with certain proprioception-related neurological disorders, such as those who suffer from abnormal sensations.

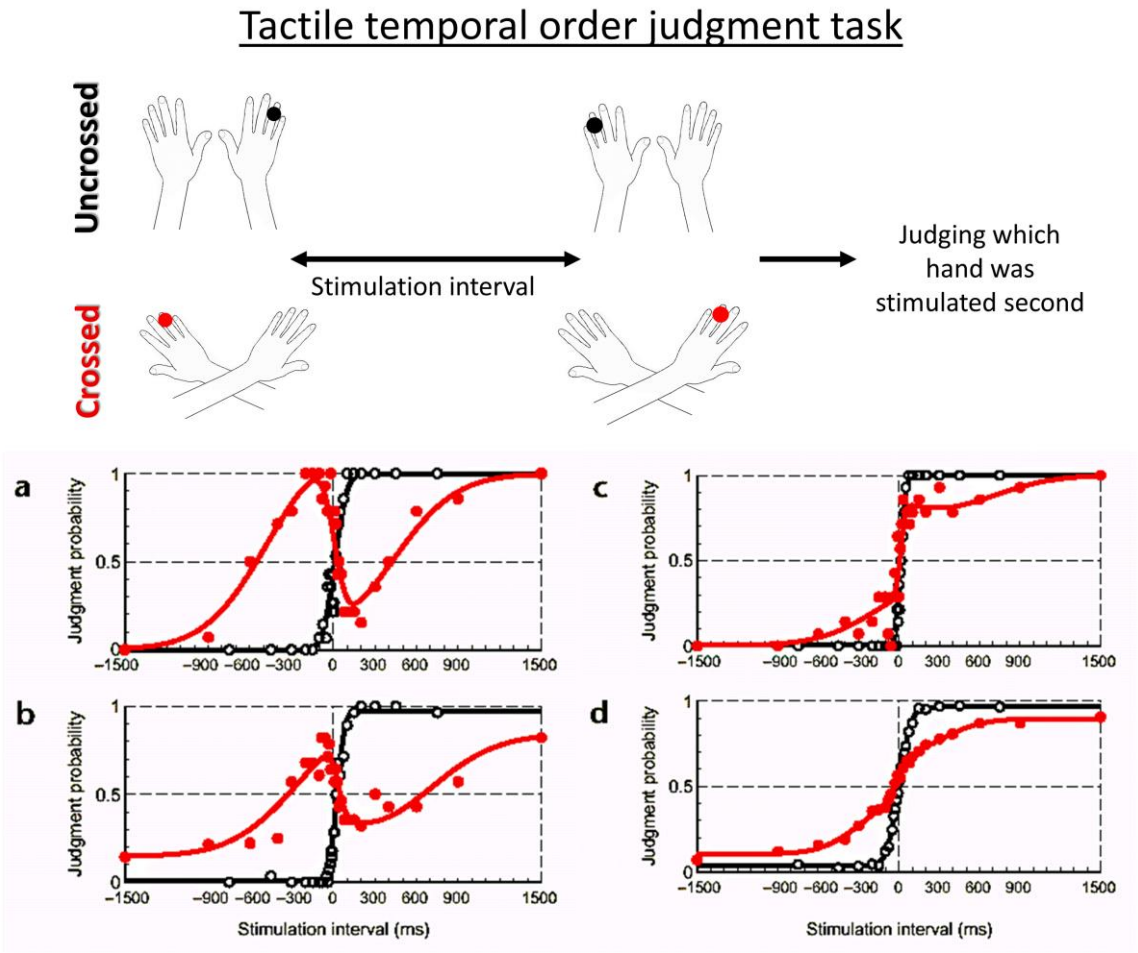

Fig. 0-1. Illustration of the tactile temporal order judgment task and the crossing effect. Two successive tactile stimuli were delivered to each hand either in a crossed or uncrossed posture, and participants were asked to judge their temporal order by identifying the second stimulus. (a-c) The order judgment probability (i.e., the probability of judging the left hand as the hand being stimulated second) against the stimulation interval in three individual subjects in the crossed (red) and uncrossed (black) postures. (d) The average of the judgment probability in twenty subjects. The negative and positive intervals correspond to the left- then right-hand stimulation and right- then left-hand stimulation, respectively. This figure shows that crossing the hands significantly affects the temporal order judgment (causes a significant number of inverted judgments). **(adapted from Yamamoto S and S Kitazawa 2001)**

Psychophysiological studies have revealed that when the hands are crossed, our brain initially senses the touch on the wrong hand, and then maps it to the correct hand (Groh JM and DL Sparks 1996; Azañón E and S Soto-Faraco 2008; Overvliet KE et al. 2011). When participants were asked to make an immediate saccade toward a stimulation delivered to their hands crossed, at first, their saccade went toward the wrong hand and then quickly curved back toward the correct hand (Groh JM and DL Sparks 1996; Overvliet KE *et al.* 2011). Similarly, in a tactile-visual task (tactile preceding the visual stimulus), it has been observed that when the hands were crossed, initially, the tactile stimulus facilitated the reaction toward a visual target presented on the opposite side; however, later, it facilitated the reaction when they were on the same side. The time-course in the curved saccadic movement and the tactile-visual task suggest that it takes around 200~400 ms for the correct mapping of a tactile stimulus to accomplish. It has been suggested that there are two reference frames in our brain associated with the spatial coordinate of a touch: anatomical and external frames. The anatomical frame is based on the somatosensory information and the default posture of the hands (i.e., the right space corresponds to the right hand, and the left space corresponds to the left hand). The external frame is constructed based on the integration of the somatosensory and spatial postural information. When the hands are crossed, the anatomical and external frames contradict each other (Fig. 0-2).

However, the exact mechanism that causes the crossing effect is still controversial and not established (Heed T and E Azanon 2014). For example, in one account, it has been hypothesized that the anatomical frames of two successive tactile stimuli induce an inverted sense of motion. Then, integration of this motion signal with the external frame causes the judgment reversal (Kitazawa S et al. 2008). In another account, it has been proposed that both anatomical and external frames are concurrently available and active. Thus, an incorrect integration of the frames (i.e.,

more weight on the anatomical frame) causes the judgment reversal (Shore DI *et al.* 2002). Further studies have suggested that this integration should be subjected to top-down control (influence of high-level functions, like attention, task expectations, and etc., on low-level functions, here the integration of the frames) (Badde S et al. 2014, 2016). One evidence for the top-down control is that the task instruction affects the judgment reversal (Badde S *et al.* 2016). For example, participants performed better when they were instructed to localize the first stimulus and ignore the second one, as compared to when they were instructed to report the temporal order by identifying the first stimulus. The other evidence is the influence of a concurrent cognitive load (Badde S *et al.* 2014). It has been observed that the crossing effect was smaller when participants performed a dual-task consisting of a memory task preceding the tactile temporal order judgment (TOJ) task.

Moreover, it has not been well established what the neural basis of the judgment reversal is. Thanks to the functional magnetic resonance imaging (fMRI) studies (Takahashi T et al. 2013; Crollen V et al. 2017), we have some ideas regarding which brain regions are involved in the crossed-hand TOJ task. In short, the previous fMRI studies reported that adopting a crossed posture activated the posterior parietal areas of the brain (Wada M et al. 2012). Furthermore, in the tactile TOJ task, the activity of some posterior regions (the superior parietal lobule, supramarginal gyrus, and precuneus), middle and superior temporal gyrus, and prefrontal cortices was stronger when the hands were crossed than uncrossed (Takahashi T *et al.* 2013; Crollen V *et al.* 2017). However, we still don't know their exact functionality and their interactions with each other. More importantly, due to methodological limitations of the fMRI, such as the low temporal resolution or dependency on the choice of control tasks, there is a great chance that some areas have been overlooked and escaped from being discovered.

Taken together, neural bases or neural mechanisms of the crossing effect still remained elusive. In the present thesis, I aimed at elucidating the neural bases and mechanism of the crossing effect. To this end, I first paid attention to great variability in the degree of judgment reversal across different individuals. On one side of the spectrum, we can find the people who have a large degree of judgment reversal (e.g., Fig. 0-1a), and on the other side, the people who show a small degree of reversal (e.g., Fig. 0-1c). I expected that the brain regions responsible for the inter-individual variability should play a major role in the crossing effect. In the first chapter of the thesis, by analyzing the structural MRI image of different individuals, I examined which brain regions and their cortical characteristics contribute to having a greater degree of reversal. I will show that there are ten regions responsible for the inter-individual variability.

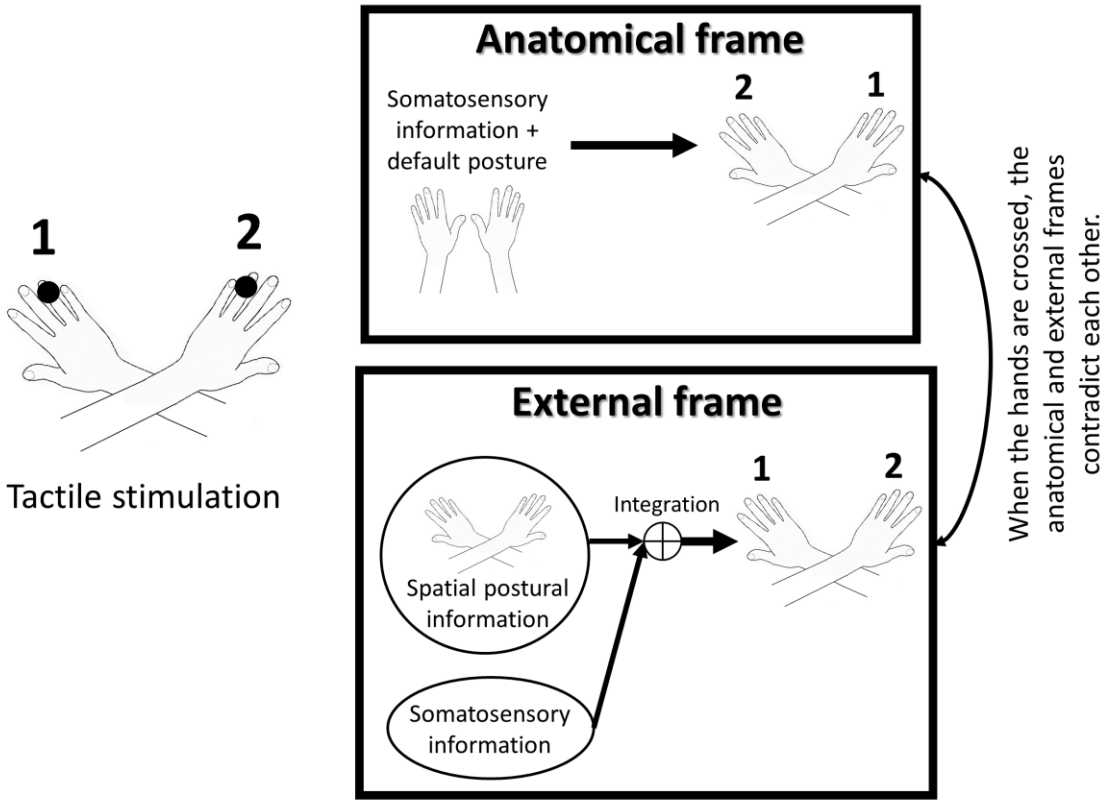

Fig. 0-2. Graphical illustration of the anatomical and external frames in a crossed-hand posture.

Even if we know these key regions that explain the crossing effect, we still don't know how they interact across time and frequency to yield inverted judgments in some trials but correct judgments in others. In the second chapter, I thus analyzed magnetoencephalographic (MEG) data, which is superior in temporal resolution than the structural or functional MRI data. By analyzing the MEG data, I found that there were two distinct modes in the brain network, one in the low-alpha frequency band (5~10 Hz) and another in the low-beta band (12~18 Hz). I will show how these two modes of network activity correspond to making a correct or inverted judgment.

Chapter 1: What underlies a greater reversal in tactile temporal order judgment when the hands are crossed? A structural MRI study

Abstract

Our subjective temporal order of two successive tactile stimuli delivered one to each hand is often inverted when our hands are crossed. However, there is great variability among different individuals. I addressed the question of why some show almost complete reversal, but others show little reversal. To this end, I obtained structural MRI data from 42 participants who also participated in the tactile temporal order judgment (TOJ) task. I extracted the cortical thickness and the convoluted surface area as cortical characteristics in 68 regions. I found that the participants with a thinner, larger, and more convoluted cerebral cortex in ten regions, including the right pars-orbitalis, right and left postcentral gyri, left precuneus, left superior parietal lobule, right middle temporal gyrus, left superior temporal gyrus, right cuneus, left supramarginal gyrus, and right rostral middle frontal gyrus showed a smaller degree of judgment reversal. In light of major theoretical accounts, I suggest that cortical elaboration in the aforementioned regions improve the crossed-hand TOJ performance through better integration of the tactile stimuli with the correct spatial representations in the left parietal regions, better representation of spatial information in the postcentral gyrus, or improvement of top-down inhibitory control by the right pars-orbitalis.

Introduction

If we are asked to judge the temporal order of two successive tactile stimuli delivered one to each hand, we often make more inverted judgments when our hands are crossed than when they are not crossed (Yamamoto S and S Kitazawa 2001; Shore DI *et al.* 2002). The finding has clearly shown that our brain cannot solely rely on somatotopic locations of the stimuli in judging their temporal order. It is already 20 years from the initial reports, but there still remain controversies over two fundamental questions.

The first question is regarding why and how the inverted judgment occurs. Different theoretical accounts have been proposed to address this question (Kitazawa S *et al.* 2008; Heed T and E Azanon 2014; Maij F et al. 2020). Kitazawa S *et al.* (2008) proposed that inverted judgment takes place because a stimulus to one hand in the crossed posture is initially mapped to the wrong hand in space, which will be remapped to the correct hand thereafter in 200~400 ms (Kitazawa S 2002). This process of remapping from the wrong to the correct hand was initially proposed based on the time course of a curved somatosensory saccade (Groh JM and DL Sparks 1996), but later confirmed by an ingenious psychological experiment (Azañón E and S Soto-Faraco 2008). Kitazawa S *et al.* (2008) further proposed that the erroneous initial mappings are fixed as an inverted motion signal when two stimuli are successively delivered before the correct remapping is achieved, with a stimulus onset asynchrony of 200 ms for example. This inversion in the motion signal was suggested as a cause of an inverted judgment. Involvement of the motion signal was supported later by a functional imaging study (Takahashi T et al. 2013). Another account was put forth by Shore et al (Shore DI *et al.* 2002). They proposed that the two external (spatial) and anatomical representations are concurrently available, thus, in the crossed posture, each hand will have two active left and right spatial characteristics. Integration of these contradictory spatial

information may lead to associating incorrect hands with the tactile stimuli. Following this thread, Badde S et al. proposed that the integration of the two representations is subject to top-down control as they found that the performance in tactile temporal order judgment (TOJ) task was modulated by the task instruction (Badde S *et al.* 2016) and by a concurrent cognitive load (Badde S *et al.* 2014). More recently, Maij F *et al.* (2020) proposed that the TOJ performance does not rely on the external representation. They suggested that the external representation will be constructed post-hoc on demand after making a hand choice, which depends on different categorical features of touch such as limb type and body side (Badde S et al. 2019). In this account, inverted judgment occurs solely due to associating an incorrect hand with a tactile stimulus upon occurrence.

The second question concerns variabilities across participants. Due to crossing of the hands, some individuals show almost complete judgment reversal, but others show much less reversal (e.g., Yamamoto and Kitazawa, 2001). The most evident factor reported thus far is the sex of participants. Generally, female participants show greater judgment reversal than male participants (Cadieux ML et al. 2010). However, there remains considerable diversity in the degree of judgment reversal even within male or female groups. In addition, the sex difference has been observed in only a few number of tactile TOJ studies (Unwalla K et al. 2020). It is possible that sex is not a primary factor but that there exist some critical parameters in the cortical structure that explain the variability in both males and females.

In the present study, I aimed to search for such parameters in the cortical structure that would explain the inter-individual variability in the degree of judgment reversal. For this purpose, I examined the brain structure of 42 participants (23 males and 19 females) and extracted the cortical thickness and the surface and mean curvature of the white-gray matter boundary in 68 anatomical

regions. Here, I show that a combined index of cortical features in a few regions explains the degree of judgment reversal regardless of the sex of the participants. Furthermore, I discuss the implications of the mechanisms of judgment reversal.

Methods

Participants

Forty-two volunteers (23 males and 19 females with an average age of 22.7 and a standard deviation of 2.1 years old) participated in this study. Thirty-nine of them were right-handed (laterality quotient between 70 and 100 with an average of 94.7 and a standard deviation of 7.3), two of them were right-hand-preferred ambidextrous (laterality quotient of 10 and 15), and one of them was left-hand-preferred ambidextrous (laterality quotient of -50) according to the Edinburgh Inventory test (Oldfield RC 1971). All participants were neurologically normal and provided written informed consent according to the guidelines of the Ethical Review Board of Osaka University, Graduate School of Frontier Biosciences.

Tactile TOJ experiment

Participants sat behind a desk, with their head fixated on a chinrest, and placed their hands on the desk (palms facing down) with their arms either crossed or uncrossed (Fig. 1-1 A). The distance between the ring fingers was kept at 20 cm in both of the postures. Participants closed their eyes and put on earphones that played white noise. They could only rely on their tactile sense. By using mechanical vibrators, two brief successive tactile stimuli were delivered one to the ring finger of each hand. Participants were asked to judge the order of the stimuli by indicating which stimulus was delivered second. Two buttons were placed under the index finger of each hand. Participants expressed their judgment by pressing those buttons. Participants were instructed to respond as soon as they received the second stimulus (within 3 s). If they responded before the delivery of the second stimulus or after the 3 s response window, the trial was considered a miss, and it would be repeated again randomly at some point throughout the session. To prevent participants from making premature judgments based on the first stimulus, in some random trials,

both stimuli were delivered to the same hand (catch trial). In the catch trials, participants were required to respond to the second stimulus as in the other trials. The catch trials were essential to make the participants pay attention to the order of the two stimuli. Otherwise, participants could focus on the perception of the first stimulus in particular, and then respond by the other hand without paying any attention to the second stimulus. I conducted the experiment in two sessions on the same day with a short break (5~10 min) in between. In the first session, the hands were parallel (uncrossed). In the second session, the hands were crossed.

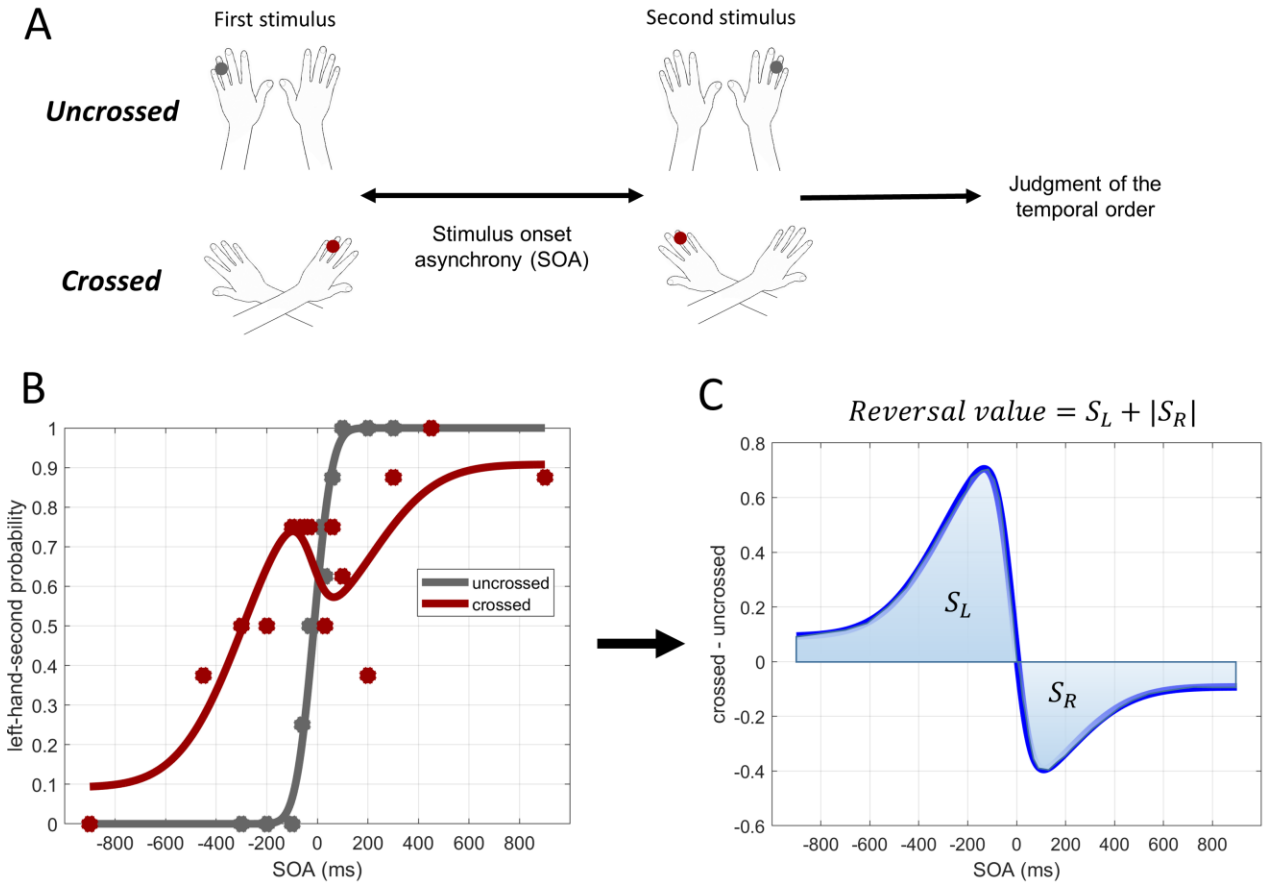

Fig. 1-1. (A) Experimental paradigm. Two successive tactile stimuli were delivered one to the ring finger of each hand, and participants were asked to judge their temporal order by identifying which hand was stimulated second. The experiment was conducted in two sessions: in the first session, the hands were parallel (uncrossed), and in the second session, the hands were crossed. (B) Left-hand-second judgment probability of one particular participant in the crossed (red) and uncrossed (gray) conditions. SOA is the

stimulus onset asynchrony of the two tactile stimuli. Positive and negative SOAs indicate that the order of stimuli was from the right- to left-hand and from the left- to right-hand, respectively. (C) The difference between the judgment probabilities in the crossed and uncrossed conditions (blue curve) shows the judgment reversal that occurred due to the crossing of the hands. The surface area of judgment reversal was used as a measure to quantify the performance of the participants in the crossed hand condition.

The stimulus onset asynchrony (SOA) of the two tactile stimuli was randomly assigned from 12 intervals (±15, ±30, ±60, ±100, ±200, ±300 ms) in the uncrossed session and from 14 intervals (±30, ±60, ±100, ±200, ±300, ±450, ±900 ms) in the crossed session. Negative and positive SOAs indicated that the order of stimuli was from the left- to right-hand (LR) and from right- to left-hand (RL), respectively. Note that since the task is more difficult in the crossed session, longer SOAs were included to properly sample the entire spectrum of performance. In both of the sessions, the SOA of the catch trials was fixed at 100 ms (+100 ms: RR, -100 ms: LL). Each SOA interval was repeated 8 times randomly. Therefore, the uncrossed session consisted of 112 trials (96 normal trials and 16 catch trials), and the crossed session consisted of 128 trials (112 normal trials and 16 catch trials). The inter-trial interval between the response (i.e., pressing the button) and the start of the next trial was randomly assigned a value between 500 and 1500 ms. Before each session, I conducted a short training session to familiarize the participants with the task.

To assess whether extracted metrics from the TOJ performances are reliably used as traits within individuals, I asked 24 of the participants (17 males and 7 females) to come again and repeat the TOJ task. Their second participation was scheduled between 3 and 12 months after their first participation. In the second participation, the conditions of the task were the same as the first participation except that the participants performed the crossed session first and then the uncrossed

session. I reversed the order of sessions in the second participation to examine whether the order has any effect on the TOJ performances.

Analysis of the TOJ data

The probability of judging the left hand as the hand stimulated second (left-hand-second judgment probability) was calculated for each SOA in the crossed and uncrossed conditions. Fig. 1-1B shows these probabilities (red and gray points) in one individual. It has been proposed that the judgment probability follows a sigmoid-shaped pattern (Eq. 1-1) in the uncrossed condition and an N-shaped pattern (Eq. 1-2) in the crossed condition (Yamamoto S and S Kitazawa 2001; Wada M et al. 2004).

$$P_u(SOA) = (P_{max} - P_{min}) \int_{-\infty}^{SOA} \frac{1}{\sqrt{2\pi}\sigma_u} e^{-\frac{(\tau - d_u)^2}{2{\sigma_u}^2}} \mathrm{d}\tau + P_{min} \quad (1\text{-}1)$$

Eq. 1-1 consists of one Gaussian cumulative distribution function that makes a sigmoid-shaped curve. P_u is the left-hand-second judgment probability in the uncrossed condition, P_{max}, P_{min}, σ_u, d_u, and SOA are the upper and lower asymptotes, the wideness, the horizontal translation, and the stimulus onset asynchrony, respectively.

$$P_c(SOA) = f_l(SOA)[1 - P_u(SOA)] + [1 - f_r(SOA)]P_u(SOA) \quad (1\text{-}2)$$

$$\begin{cases} f_l(SOA) = A_l e^{-\frac{(SOA-d)^2}{2{\sigma_f}^2}} + c \\ f_r(SOA) = A_r e^{-\frac{(SOA-d)^2}{2{\sigma_f}^2}} + c \end{cases}$$

Eq. 1-2 consists of two up and down Gaussian flips (f_l and f_r), one on each side of the y axis, making an N-shaped curve. P_c is the left-hand-second judgment probability in the crossed condition; A_l and A_r are the peaks of the up and down flips, respectively; and σ_f, d, and c are the width, the horizontal translation, and the vertical translation of the flips, respectively. The variables

in Eqs. 1-1 and 1-2 were calculated by using the maximum likelihood estimation and the MATLAB optimization toolbox. Figure 1-1B shows the fitted curves in one individual. Note that the purpose of these curve fittings is to make the overall evaluation of the participant's performance more robust and reliable. The model was not rejected in 38 out of the 42 participants by the goodness of fit test using the Pearson's chi-square statistic ($p > 0.05, \chi^2 < 15.5$, $df = 8$ in the crossed condition and $\chi^2 < 14.1$, $df = 7$ in the uncrossed condition)(Linhart H and W Zucchini 1986). In the four cases in which data did not pass the goodness of fit test, I observed the data by the eye. I judged that the model captured essential characteristics of the data because the determination coefficient was greater than 0.4 (Fig. 1-2).

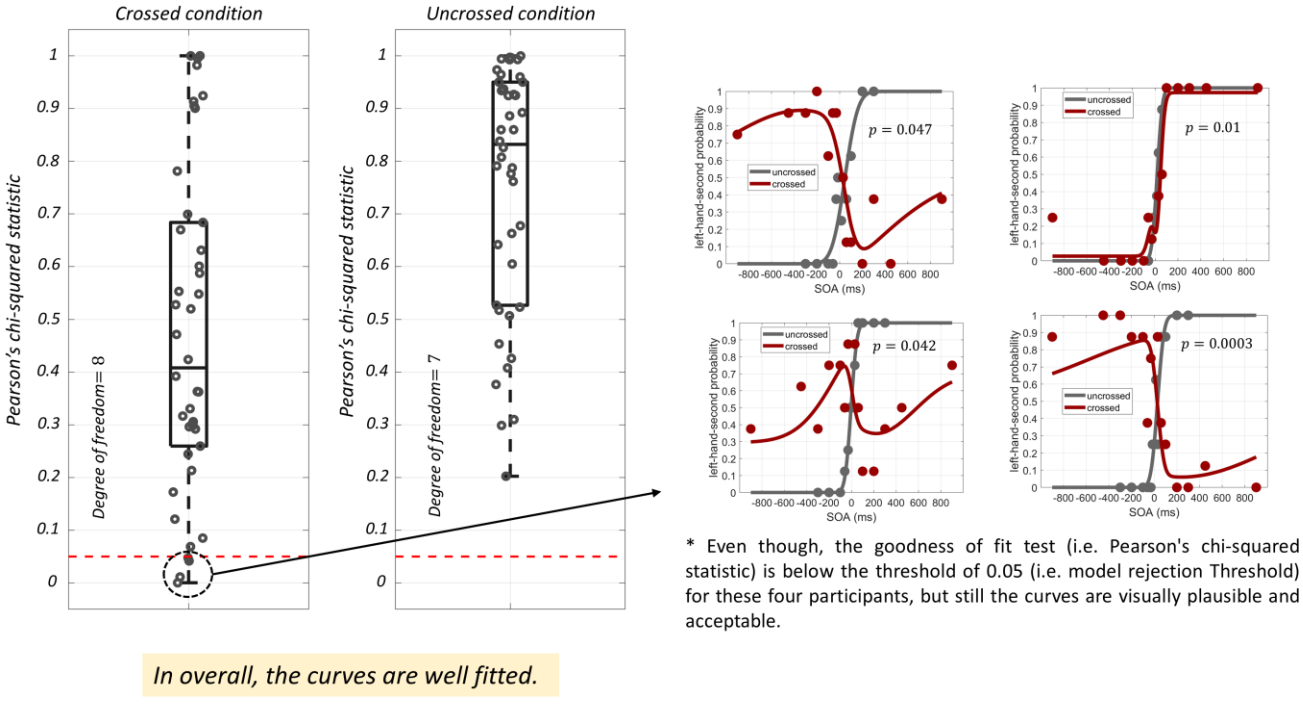

Fig. 1-2. Evaluation of the goodness of the fitted curves. Pearson's chi-squared statistic (*p*) of the fitted curves in the uncrossed (Eq. 1-1) and crossed (Eq. 1-2) conditions across participants.

By subtracting the left-hand-second judgment probability curve of the crossed condition from the uncrossed condition (Fig. 1-1C), we can observe the judgment reversal (i.e., erroneous

judgments) that occurred due to the crossing of the hands. The absolute surface area of this subtracted curve was used as a measure to quantify the degree of judgment reversal. I called this measure the reversal value. I normalized the reversal value by dividing it by its maximum possible value. The normalized reversal value ranged between 0 and 1, with 0 indicating absolutely no judgment reversal and 1 indicating a complete judgment reversal over all of the SOAs. To test which aspects of the flip model were reflected in the reversal value, I examined correlations between the reversal value and the model parameters in Eq. 1-2 (A_l, A_r, σ_f, and c).

Structural MRI acquisition

T1-weighted structural MRI images were acquired using 3-Tesla MRI scanners. Twelve of the participants were scanned with a MAGNETOM Vida (MP-RAGE sequence), and the other thirty were scanned with a MAGNETOM Prisma, Siemens scanner (gradient-recalled echo/inversion recovery sequence). Note that the resolution of the MRI images acquired from the two scanners was the same (slice thickness = 1 mm, repetition time (TR) = 1900 ms, echo time (TE) = 3.37 ms, flip angle (FA) = 9 degrees, field of view (FOV) = 256×256 mm, and voxel size = 1×1×1 mm).

One of the participants was scanned by both scanners. The participant was scanned first with the Vida scanner, and after 3months, with the Prisma scanner. I compared the data of the two scanners to check whether there was any scanner bias affecting the analyses.

Analysis of the structural MRI images

I used FreeSurfer software to analyze the structural MRI images (Fischl B 2012). FreeSurfer finds the white-gray matter boundary and makes its 3D surface model using triangular meshes (approximately 150,000 vertices per hemisphere) (Dale AM et al. 1999). The meshes of triangles allow measuring the surface area, curvature and cortical thickness at each vertex. The surface area

of a vertex is the sum of the areas of its surrounding triangles divided by three. The cortical thickness of a vertex indicates its distance to its corresponding closest point on the pial-cerebrospinal fluid surface. Each vertex has two principal curvatures (k_1 and k_2), which measure the maximum and minimum bending. The average value of k_1 and k_2 is known as the mean curvature (H) (Pienaar R et al. 2008; Ronan L et al. 2011).

FreeSurfer automatically parcellates the cerebral cortex into 68 standard gyral-based anatomical regions (34 regions per hemisphere) known as the Desikan-Killiany atlas (Fischl B et al. 2004; Desikan RS et al. 2006). I used those 68 regions to compare the structural properties of individual brains.

In choosing structural properties for analyses, I paid particular attention to those that have been reported to correlate with intelligence in young participants as recruited in the present study (Luders E et al. 2009; Schnack HG et al. 2015; Tadayon E et al. 2020). I expected that such properties would be linked with cortical elaboration, or efficiency, which would have critical effects on the complex process of judgment reversal. It has been reported that cortical curvature and surface area correlated positively with intelligence whereas cortical thickness correlated negatively (Luders E *et al.* 2009; Schnack HG *et al.* 2015; Tadayon E *et al.* 2020). This motivated defining a measure that combines curvature and surface area that would reflect a kind of cortical efficiency or elaboration. The measure, termed rectified surface integral (RSI), was defined as follows:

$$RSI = \sum_{A} |H| dA \tag{1-3}$$

where H is the mean curvature, dA is the surface area, and A refers to the vertices of one anatomical region. The RSI emphasizes the surface area (dA) with a greater curvature (H) but ignores a flat surface. I expected that the RSI would provide a more reliable measure of cortical

elaboration than a simple sum of the surface areas. To make the RSI robust to spatial distortions, I used a spatially smooth version of the mean curvature values produced by FreeSurfer in its analysis pipeline. I then defined the mean cortical thickness (MCT) by the following equation:

$$MCT = \frac{\sum_A T}{N_A} \tag{1-4}$$

where T is the cortical thickness, and N_A is the number of vertices of one anatomical region. I further introduced the ratio of RSI to MCT (RSI/MCT) in an expectation that it would serve as a more sensitive positive measure of cortical elaboration. I also examined the gray matter volume, because a recent study reported that fluid intelligence was associated with the parameter (Chen PY et al. 2020).

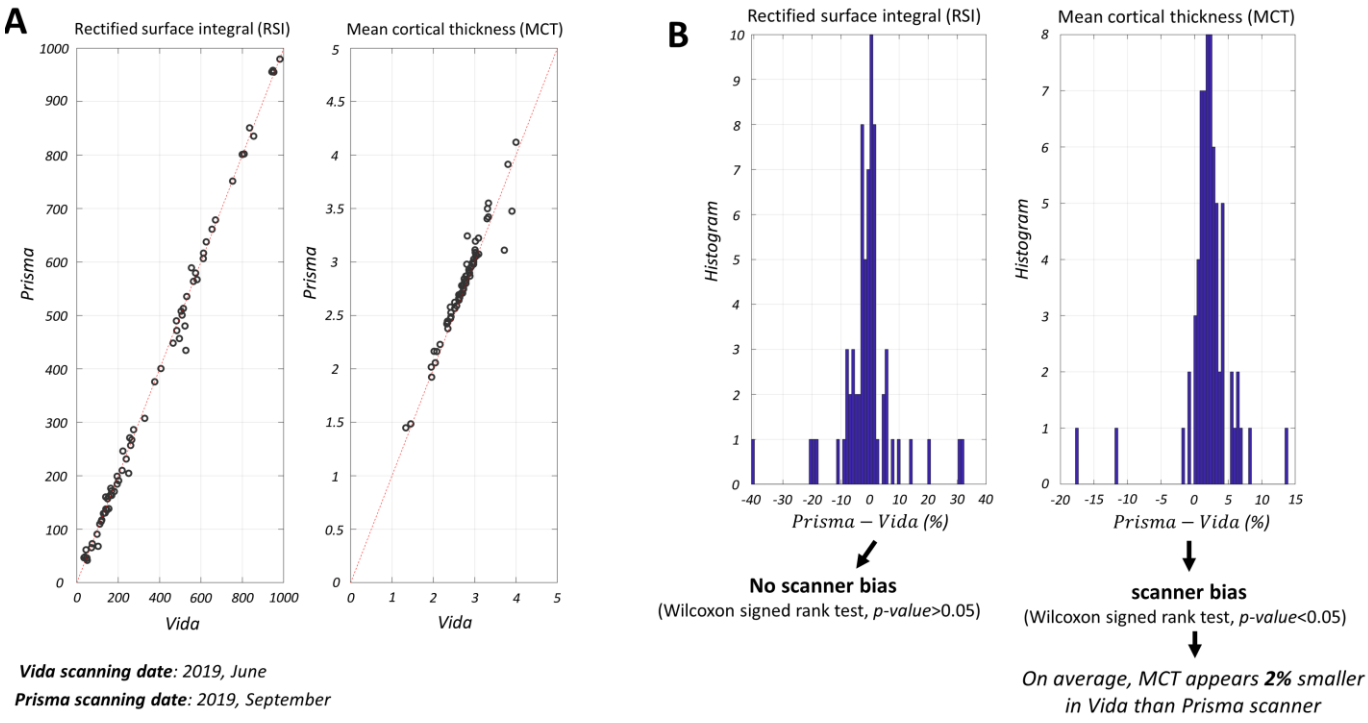

Fig. 1-3. Evaluation of the Vida and Prisma scanners compatibility. (A) Cortical measures (i.e., RSI and MCT) of the 68 anatomical regions acquired from the MRI images of one particular participant scanned by the Vida and Prisma scanners. (B) Histogram of the percentage difference between the acquired cortical measures by the Vida and Prisma scanners.

I tested whether there was any scanner bias by comparing data of the one participant who was scanned by both scanners. There was no scanner bias in the RSI, but there was a significant scanner bias in the MCT. On average, MCT was 2% smaller in the Vida than the Prisma scanner (Fig. 1-3). This small difference was reasonable because the cortical thickness was reported sensitive to scanner types (Iscan Z et al. 2015). I confirmed that a correction of the MCT by 2% in the 12 participants who were scanned by the Vida scanner did not alter the basic findings in the present study. As there was no bias in the RSI and the bias in the MCT was small (2%), the data of the Prisma and Vida scanners were analyzed together.

I examined the correlation between each of the cortical measures (i.e., MCT, RSI, and RSI/MCT) and the reversal value. As there were 68 anatomical regions and subsequently 68 correlation values, to find the significant regions, I corrected the *p*-values for multiple (i.e., 68) tests by using the Benjamin-Hochberg false discovery rate (FDR) (Benjamini Y and Y Hochberg 1995). I repeated the same correlation analyses by using the mean of A_l and A_r (mean peak flip), which would reflect the pure degree of judgment reversal in TOJ, instead of the reversal value.

Finally, I searched for a model that could effectively estimate the reversal value from the cortical characteristics.

$$Reversal\ value \sim g\left(\sum_{i=1}^{N} \propto_i F_i + C\right) \tag{1-5}$$

$$g(z) = \int_{-\infty}^{z} \frac{1}{\sqrt{2\pi}} e^{-\frac{x^2}{2}} dx \tag{1-6}$$

The model was made up of a linear combination of the cortical characteristics (F_i) passing through a normal cumulative distribution function (g) (Eqs. 1-5 and 1-6, Fig. 1-10A). The normal cumulative distribution function was adopted to make the output of the model fall between 0 and 1, within the range of the reversal value. Moreover, it can improve the model by accounting for a

possibly existing nonlinearity between the cortical characteristics and the reversal value. By testing the model with and without the nonlinear layer (i.e., Normal cdf), I realized that the nonlinearity of the model was beneficial. Basically, after identifying the cortical characteristics that had significant correlation with the reversal value, I tried all possible combinations of one, two, three, and up to eight of those cortical characteristics in the model. In addition to the cortical characteristics, I considered sex as a factor in the model to assess its possible significance. The Stan programming language (Carpenter B et al. 2017) was used to fit the model to the data. I employed the leave-one-out (LOO) cross-validation (Vehtari A et al. 2017) to find the most effective model (i.e., the combination of cortical characteristics that could effectively explain the reversal value). Moreover, I calculated Pareto k, an estimate of the distance between an individual leave-one-out distribution and the full distribution. A Pareto k greater than 0.7 suggests that the left-out data was an outlier and that the model was not adequate. The model with the lowest LOO information criterion and with all 42 Pareto k values smaller than 0.7 was selected as the best model (Fig. 1-10B).

*Data/code availability***:** The data that support the findings of this study are openly available at http://dx.doi.org/10.17632/tfkdrc4yfw.1 (Moharramipour and Kitazawa, 2020).

Results

In the uncrossed condition, the participants generally responded correctly when the SOA was greater than 100 ms (e.g., gray sigmoid curve in Fig. 1-1B). By contrast, in the crossed condition, the participants often showed inverted judgment even with SOAs greater than 200 ms (e.g., N-shaped response curve in Fig. 1-1B). However, it is noteworthy that the degree of judgment reversal varied considerably across the participants (Fig. 1-4A). Some participants showed nearly complete reversal (e.g., inverted sigmoid, top right panel in Fig. 1-4A) or N-shaped response curves (e.g., right middle panel in Fig. 1-4A), but others made much fewer inverted judgments (e.g., left top and left middle panels in Fig. 1-4A). The female participants generally showed a larger reversal value than the male participants (Fig. 1-4B), but the difference was not significant (Wilcoxon rank-sum test, *p*-value = 0.23).

To summarize the crossing effect in the tactile TOJ task, I introduced the reversal value (Fig. 1-1c) which takes a value between 0 (no reversal) and 1 (full reversal). I confirmed that the reversal value correlated significantly with most of the parameters in the flip model of Eq. 1-2 (Fig. 1-5). It correlated significantly with the peak probability of the flips ($A_l: r = 0.56$, $A_r: r = 0.50,\ p < 0.001$) and their mean ($(A_l + A_r)/2: r = 0.75,\ p < 10^{-7}$), which reflect the peak probability of judgment reversal. It was also highly correlated with the affected time window ($\sigma_f: r = 0.93, p < 10^{-18}$), and the general spatial error ($c: r = 0.92,\ p < 10^{-17}$). The reversal value could thus be regarded as a comprehensive measure of the crossing effect.

Data of those 24 participants who performed the task for the second time revealed that the TOJ performance was highly reproducible (Fig. 1-6). The reversal values of their first and second participations were highly correlated with each other ($r = 0.95$). The other model parameters also showed significant correlations (0.60, 0.70, 0.86, and 0.95 for A_l, A_r, σ_f, and c). The results agree

with a recent report that the crossed-hand effect was highly reproducible within each individual participant (Unwalla K *et al.* 2020).

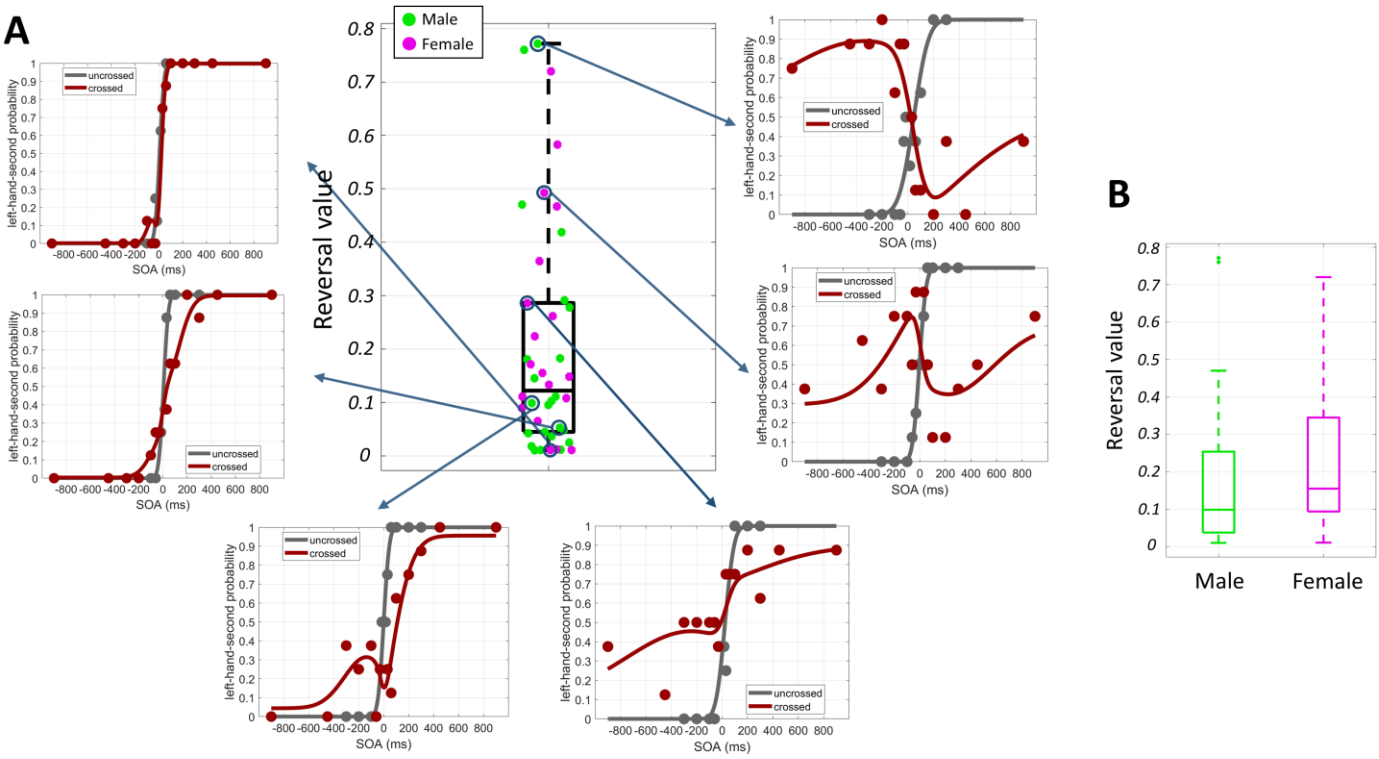

Fig. 1-4. (A) Reversal values of the participants. Reversal values range between 0 and 1. Zero indicates absolutely no reversal, and one indicates complete reversal. A lower reversal value corresponds to a better performance in the crossed hand tactile temporal order judgment (TOJ) task (Fig. 1-1A). The judgment probabilities of the crossed and uncrossed conditions are shown for some reversal values. When the reversal value is lower, the difference between the crossed and uncrossed conditions is smaller. Male and female participants are shown with green and magenta colors, respectively. (B) Reversal values of the male and female participants. On average, females showed a greater reversal value than males; however, the difference was not significant (Wilcoxon rank-sum test, *p*-value = 0.23).

The order of the crossed and uncrossed sessions was reversed in the second participation. The order did not significantly affect judgment reversal in each individual because there was no significant difference between the parameters in the first and second participations (Wilcoxon signed ranked test, $p > 0.05$). Taken together, the reversal value could be regarded as a comprehensive and reliable measure of judgment reversal in each individual participant.

Correlation between the metrics

	Reversal value	σ_f	A_l	A_r	$(A_l+A_r)/2$	c
Reversal value	1.00	0.93	0.56	0.50	0.75	0.92
σ_f	0.93	1.00	0.45	0.50	0.67	0.76
A_l	0.56	0.45	1.00	−0.014	0.79	0.50
A_r	0.50	0.50	−0.014	1.00	0.60	0.45
$(A_l+A_r)/2$	0.75	0.67	0.79	0.60	1.00	0.67
c	0.92	0.76	0.50	0.45	0.67	1.00

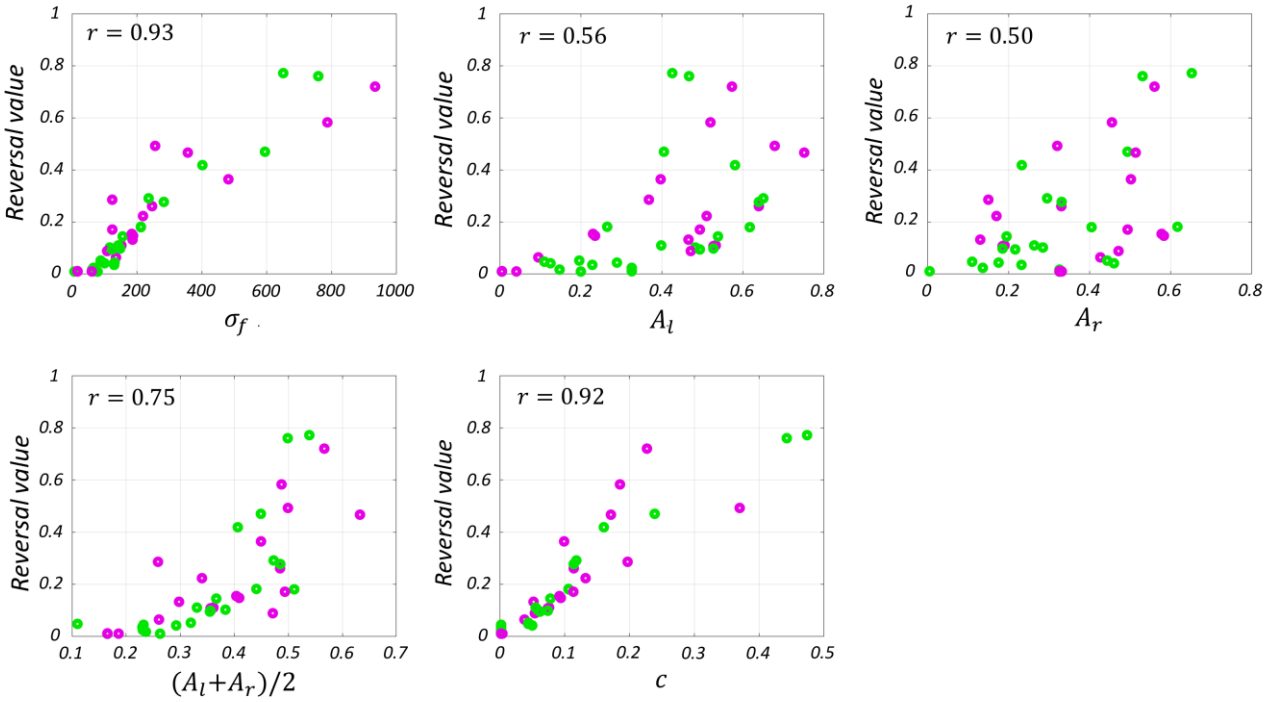

Fig. 1-5. Correlation between the parameters of the Gaussian flip model (Eq. 1-2) and the reversal value. The profile of the reversal value versus each of the parameters is shown in the subplots. Male and female participants are shown with green and magenta colors, respectively.

The MCT over the whole brain was positively correlated with the reversal value (Fig. 1-7B, $r = 0.42, p = 0.0061$). Region-by-region analyses (Fig. 1-7A, uncorrected $p < 0.05$) yielded many regions with positive correlations. After correction for the false discovery rate of 0.05 (FDR correction), the two regions of the right pars-orbitalis (i.e., orbital part of the inferior frontal gyrus)

and right rostral middle frontal gyrus were identified as significant. As shown in Fig. 1-7C, the MCT of these two regions had a strong positive correlation with the reversal value.

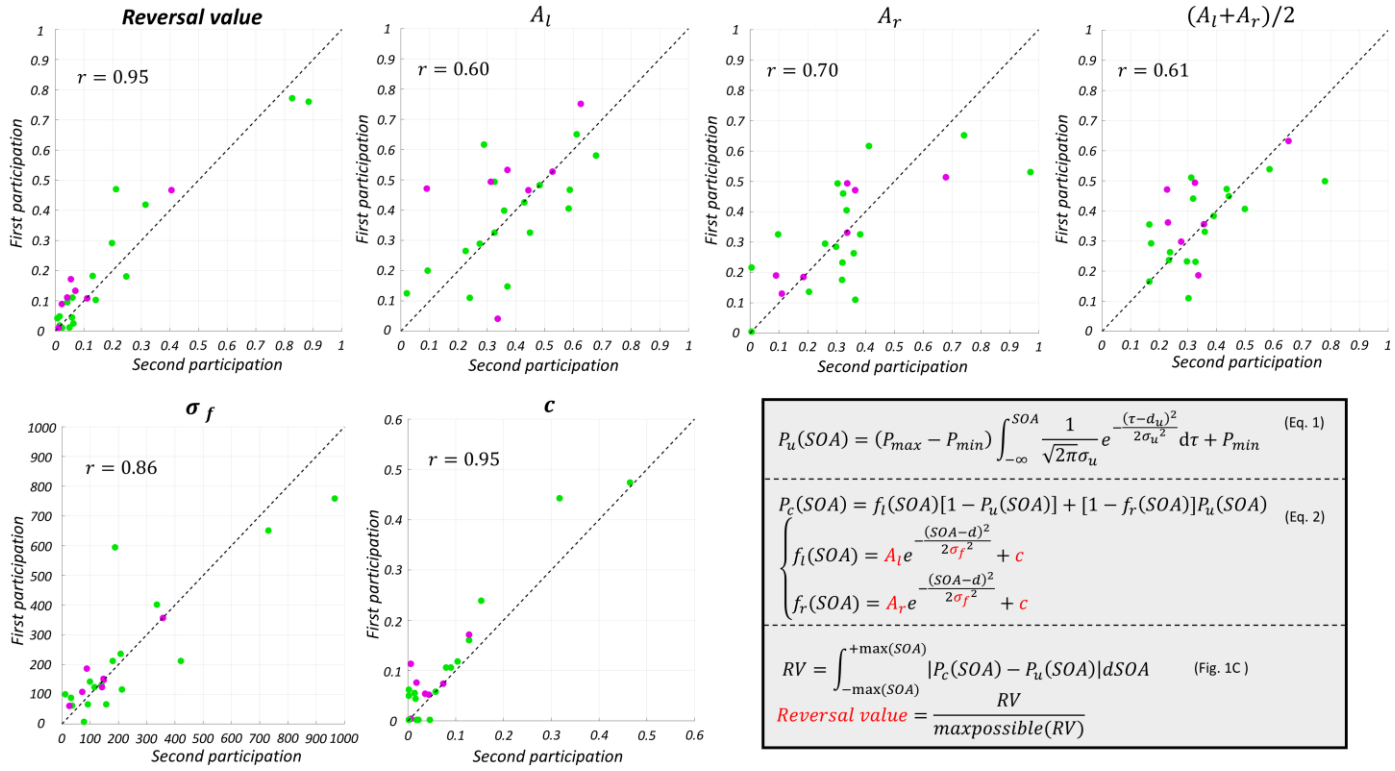

Fig. 1-6. Evaluation of the reproducibility of the TOJ performance**.** Metrics of the *reversal value*, σ_f, A_l, A_r, and c acquired from the TOJ performance of the subjects in their first versus second participations are shown in the subplots. Definition of the metrics is shown in the bottom right panel.

By contrast, the whole brain RSI was negatively correlated with the reversal value, though it did not reach the level of significance (Fig. 1-7E, $r = -0.28, p = 0.078$). The region-by-region analyses (Fig. 1-7D, uncorrected, $p < 0.05$) yielded several regions with negative correlations. After the FDR correction, the right and left postcentral gyri and the right cuneus were identified as significant (Fig. 1-7F).

As for the RSI to MCT ratio, the following eight regions were identified after the FDR correction: the right and left postcentral gyri, right middle temporal gyrus, left superior parietal

lobule, left superior temporal gyrus, left precuneus, right cuneus, and left supramarginal gyrus (Fig. 1-8C).

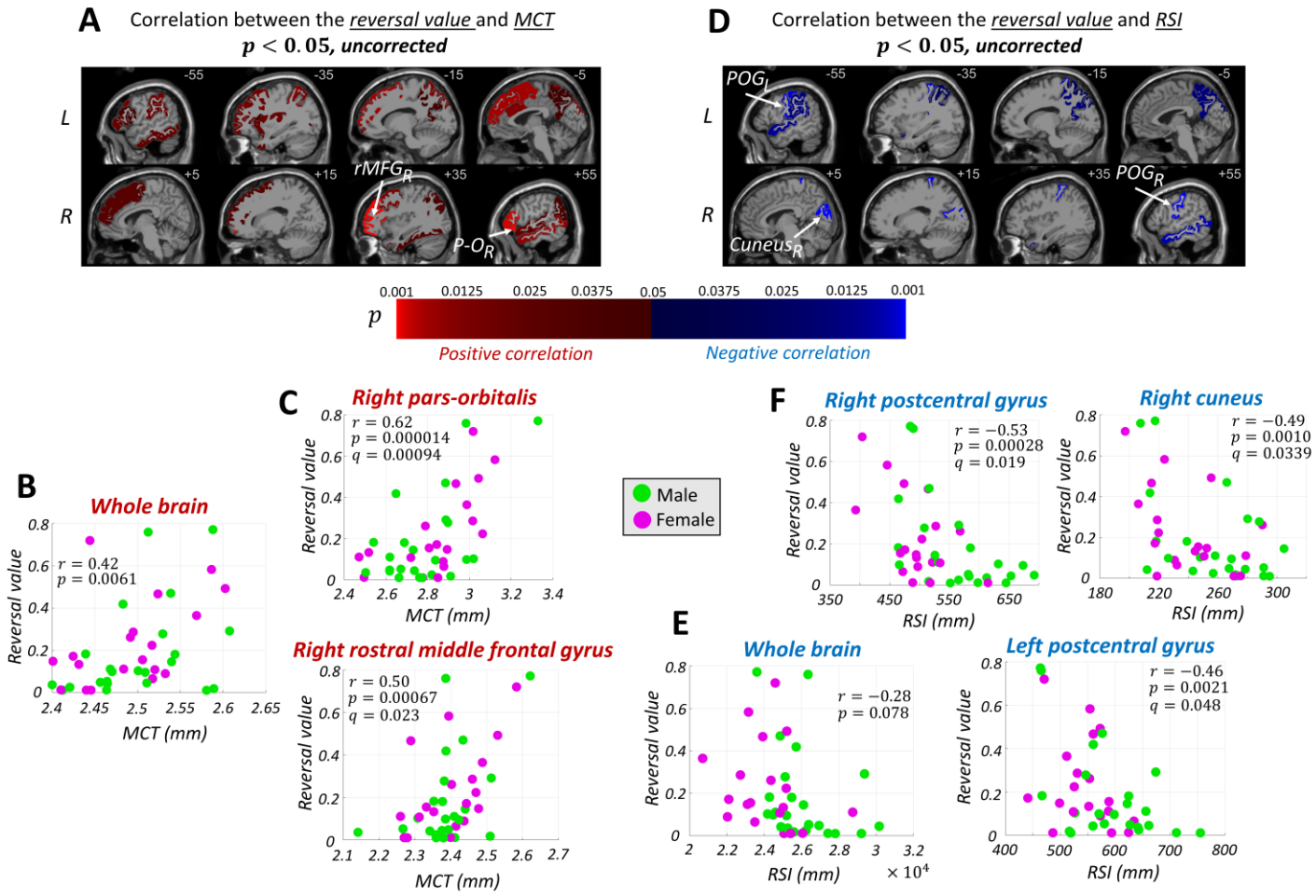

Fig. 1-7. The brain anatomical regions (according to the Desikan-Killiany atlas) whose (A) mean cortical thickness (MCT) (D) rectified surface integral (RSI) had a noticeable ($p < 0.05$, uncorrected) correlation with the reversal value. Positive and negative correlations are shown with red and blue colors, respectively. The regions with a higher correlation value (i.e., lower *p*-value) are shown with a brighter color. After correction for the false discovery of 0.05, in the MCT, right pars-orbitalis ($P\text{-}O_R$) and right rostral middle frontal gyrus ($rMFG_R$) and in the RSI, right postcentral gyrus (POG_R), right cuneus ($cuneus_R$), and left postcentral gyrus (POG_L) survive as significant. The reversal value versus the (B) MCT of the whole brain and (E) RSI of the whole brain. The reversal value and (C) MCT (F) RSI profile of the regions that passed the FDR threshold of 0.05. r, p, and q indicate the correlation value, *p*-value and *q*-value, respectively. Male and female participants are shown with green and magenta colors, respectively.

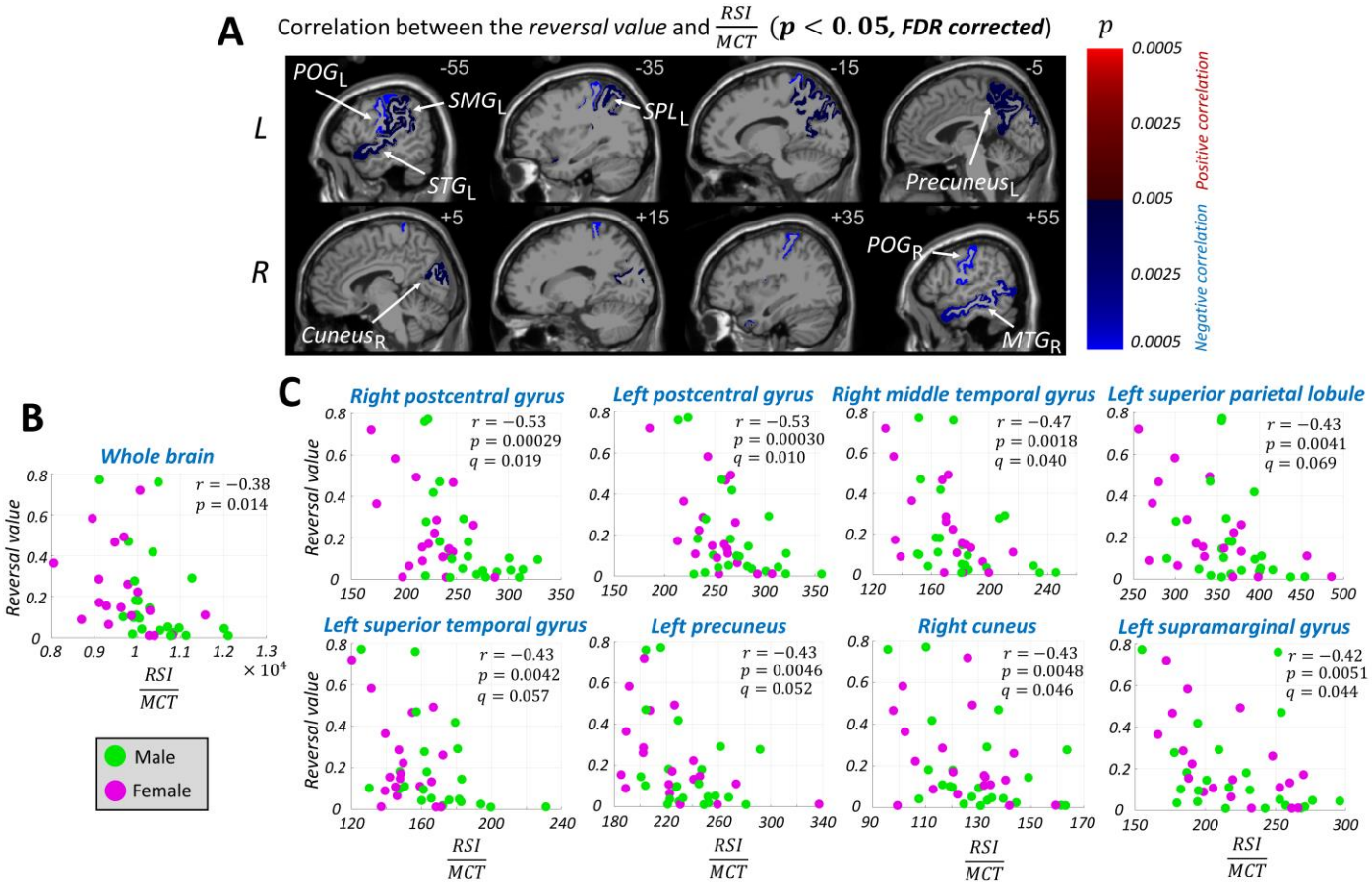

Fig. 1-8. (A) The brain anatomical regions (according to the Desikan-Killiany atlas) whose RSI to MCT ratio had a significant (p < 0.05, FDR corrected) correlation with the reversal value. Positive and negative correlations are shown with red and blue colors, respectively. The regions with a higher correlation value (i.e., lower *p*-value) are shown with a brighter color. (B) The reversal value versus the RSI to MCT ratio of the whole brain. (C) The RSI to MCT ratio and reversal value profile of the regions with a significant correlation (i.e., right postcentral gyrus (POG_R), left postcentral gyrus (POG_L), right middle temporal gyrus (MTG_R), left superior parietal lobule (SPL_L), left superior temporal gyrus (STG_L), left precuneus ($precuneus_L$), right cuneus ($cuneus_R$), and left supramarginal gyrus (SMG_L)). r, p, and q indicate the correlation value, *p*-value, and *q*-value, respectively. Male and female participants are shown with green and magenta colors, respectively

As for the gray matter volume, the correlations were generally weak and negative, with the strongest ones at the right postcentral gyrus ($r = -0.38$, $p = 0.013$), left superior temporal gyrus

($r = -0.33$, $p = 0.035$), and right entorhinal cortex ($r = -0.31$, $p = 0.042$). None of the 68 regions survived the FDR correction.

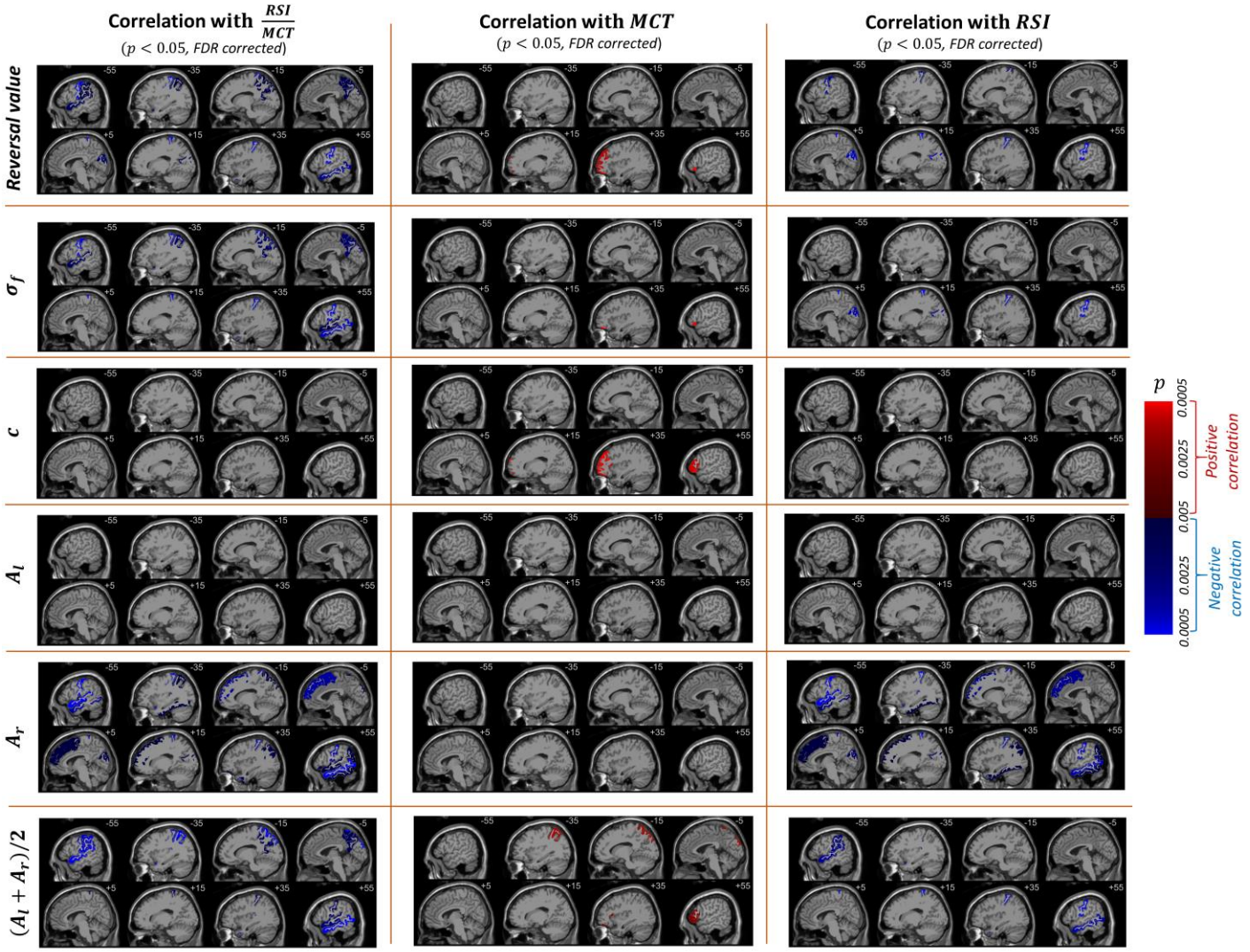

Fig. 1-9. Correlation analysis between the cortical characteristics (i.e., RSI, MCT and RSI/MCT ratio) and the metrics of the crossed-hand tactile TOJ performance (i.e., *reversal value*, σ_f, c, A_l, A_r, and $(A_l + A_r)/2$).

Table 1-1 summarizes the main findings by listing the ten brain regions that showed a significant correlation between either of the MCT, RSI, or RSI/MCT and the reversal value. When I applied the same analyses by using the mean peak flip ($(A_l + A_r)/2$) instead of the reversal value,

the major findings remained unchanged: eight of the ten regions showed significant correlation (Table 1-1, Fig. 1-9).

Last, I discovered that a model made up of the following two cortical features could most effectively explain the variability in judgment reversal (Fig. 1-10): 1) the MCT of the right pars-orbitalis, and 2) the RSI to MCT ratio of the right postcentral gyrus. It is noteworthy that the addition of sex to the model did not improve the model in terms of the leave-one-out information criterion (LOOIC, Fig. 1-10B). As shown in Fig. 1-10C, the model estimated the reversal value quite precisely ($r = 0.75$) for both male and female participants.

	Reversal value			Mean peak flip		
Brain region	MCT	RSI	RSI/MCT	MCT	RSI	RSI/MCT
Right pars-orbitalis	**0.62**	−0.064	−0.29	**0.47**	−0.14	−0.31
Right middle frontal gyrus	**0.50**	−0.23	−0.36	0.36	−0.31	−0.38
Right postcentral gyrus	0.20	**−0.53**	**−0.53**	−0.012	**−0.51**	**−0.44**
Right cuneus	0.030	**−0.49**	**−0.43**	0.064	−0.40	−0.38
Right middle temporal gyrus	0.40	−0.42	**−0.47**	0.38	**−0.48**	**−0.52**
Left postcentral gyrus	0.27	**−0.46**	**−0.53**	0.23	−0.42	**−0.49**
Left superior parietal lobule	0.38	−0.34	**−0.43**	**0.48**	−0.39	**−0.51**
Left superior temporal gyrus	0.18	−0.40	**−0.43**	0.21	**−0.47**	**−0.51**
Left precuneus	0.31	−0.38	**−0.43**	0.20	−0.42	**−0.44**
Left supramarginal gyrus	0.36	−0.38	**−0.42**	0.35	**−0.46**	**−0.50**
Whole brain	**0.42**	−0.28	**−0.38**	**0.39**	**−0.41**	**−0.50**

Table 1-1. Summary of the correlation analysis. The ten brain regions whose cortical measures (MCT, RSI, RSI/MCT) were significantly correlated (FDR corrected, $p < 0.05$) with the reversal value or the mean peak flip are listed in the rows. Numbers in bold represent the correlation values that passed the false discovery rate threshold of 0.05. MCT: mean cortical thickness, RSI: rectified surface integral, RSI/MCT: RSI to MCT ratio.

Discussion

In the current study, I examined the correlation between the structural MRI images of normal healthy individuals and their ability to perform a tactile TOJ task when their hands were crossed. I found that the cortical structural features (MCT, RSI, and RSI/MCT) of the following ten regions significantly correlated with the individuals' performance on the task: the right and left postcentral gyri, right middle temporal gyrus, left superior parietal lobule, left superior temporal gyrus, left precuneus, right cuneus, left supramarginal gyrus, right pars-orbitalis, and right rostral middle frontal gyrus (Table 1-1). Moreover, I discovered that knowing the cortical characteristics in just two of those regions, the right pars-orbitalis, and right postcentral gyrus, was essentially adequate to effectively explain the variability in judgment reversal (Fig. 1-10). It is worth noting that the addition of sex did not significantly improve the model. I did not find any significant sex difference when I directly compared the reversal value, either. Therefore, sex should not be a major affecting factor in the degree of judgment reversal. The sex difference (i.e., larger reversal in females than males) has been observed significantly in a previous study (Cadieux ML *et al.* 2010), however, a later and more inclusive research has shown that this effect was not significant
in a majority of different tactile TOJ studies (20 out of 23 studies) (Unwalla K *et al.* 2020). The present study suggests that the sex doesn't add a significant information beyond the cortical characteristics in explaining the degree of judgment reversal. Therefore, in the previous studies in which the sex difference reached the level of significance, cortical structural differences in certain anatomical regions between male and female groups can be thought of as one of the causes, besides the sex per se. Last, I discovered that in general, the participants with a thinner (lower MCT), larger and more convoluted (higher RSI) cerebral cortex in a few critical regions tended to have a smaller degree of judgment reversal in both males and females.

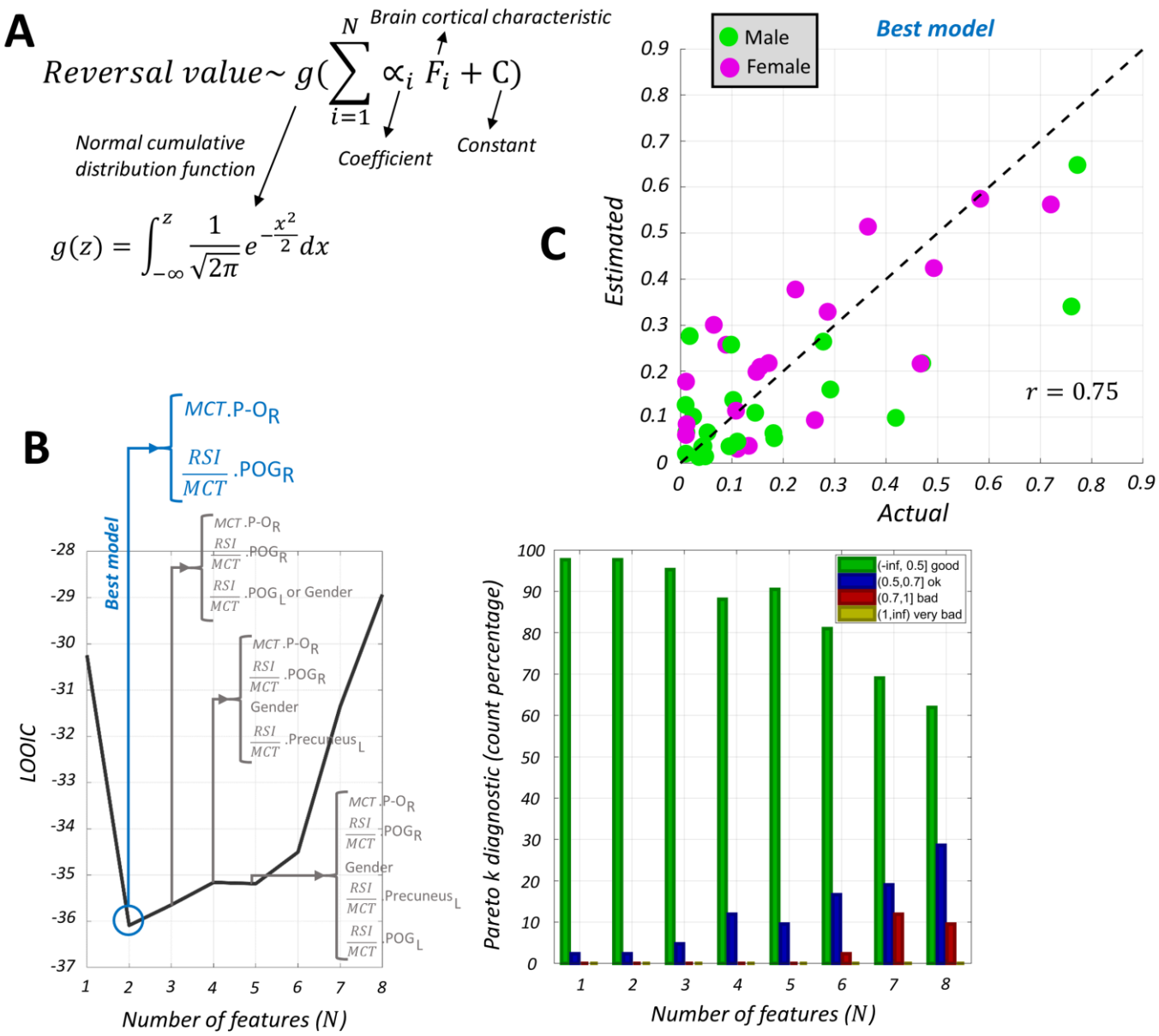

Fig. 1-10. (A) Generalized linear model with a nonlinear sigmoid function (normal cumulative distribution function) that relates the cortical characteristics to the reversal value. (B) The leave-one-out (LOO) cross-validation approach to finding the best model. Lowest achievable LOO information criterion (LOOIC) with 1, up to 8 number of features and their corresponding Pareto k values. $P\text{-}O_R$: right pars-orbitalis, POG_R: right postcentral gyrus, POG_L: left postcentral gyrus. (C) Actual reversal values versus the reversal values estimated from the best model. Male and female participants are shown with green and magenta colors, respectively.

Implications of the MCT and RSI

The MCT (thickness) correlated positively, but the RSI (convoluted surface area) correlated negatively with the reversal value. As a result, the gray matter volume, multiplication of the cortical thickness, and surface area did not show any significant correlation. It is worth discussing what a thinner, larger, and more convoluted cortex would mean regarding cortical functions, in general.

A higher cortical surface area means a higher number of cortical columns (Lübke J and D Feldmeyer 2007), which is associated with a reduction in the fraction of columnar interconnections (Ringo JL 1991). It has been proposed that a higher number of cortical columns and subsequently a smaller percentage of interconnectedness leads to higher information capacity and specialization by allowing limited interference and overlapping of information (Ringo JL 1991; Tadayon E *et al.* 2020). The increase of surface area in a certain brain region would thus lead to an increase in information capacity and more specialized functionalities carried out in that region.

As for the thickness of the cortex, we should pay careful attention to age. Cortical thickness increases in childhood (on average, until the age of ten), then goes through thinning during adolescence, more drastically in more intelligent children (Shaw P et al. 2006; Shaw P et al. 2008; Schnack HG *et al.* 2015). As far as the young adults, the age group of the present study, are concerned, a negative association between the cortical thickness and general intelligence (Schnack HG *et al.* 2015; Tadayon E *et al.* 2020), visual creativity (Tian F et al. 2018), and visual perceptual acuity (Song C et al. 2015) has been reported. Therefore, in this age group, a thinner cortex is possibly associated with a better and more efficient function. However, it is noteworthy that in older age groups, a thinner cortex might not correspond to higher efficiency, but the atrophy of the brain, as it has been reported that a younger group (20~40 years old) with higher cortical thickness

had a higher common intelligence than an older group (e.g., 50~80 years old) with lower cortical thickness (Salthouse TA et al. 2015).

Roles of the ten regions in crossed-hand TOJ

I here discuss how the ten regions listed in Table 1-1 can possibly influence one's degree of judgment reversal. It is first worth noting that the majority of the regions have been implicated for the tactile TOJ by fMRI and MEG studies (Wada M *et al.* 2012; Takahashi T *et al.* 2013; Ora H et al. 2016; Crollen V *et al.* 2017; Takahashi T and S Kitazawa 2017).

In one fMRI study, Takahashi T *et al.* (2013) investigated the neural correlates of tactile TOJ. They compared the TOJ task with the numerosity judgment (NJ) task, in both of which the same set of tactile stimuli (braille pin stimuli) were delivered to both hands. The neural correlates of TOJ (TOJ > NJ) consisted of the right middle temporal gyrus, left supramarginal gyrus, left superior temporal gyrus, and right middle frontal gyrus. In another fMRI study, Crollen V *et al.* (2017) found that the left precuneus, right middle temporal gyrus, and left superior parietal lobule were significantly activated during crossed-hand tactile TOJ compared with uncrossed-hand tactile TOJ (crossed > uncrossed). It has been found that the supramarginal gyrus plays a major role in the awareness and sense of hand position (Ben-Shabat E et al. 2015; Findlater SE et al. 2018). It was reported in a lesion study that the superior parietal lobule plays a major role in updating and maintaining the internal representation of the body (Wolpert DM et al. 1998). Thus more elaborate (more efficient) left superior parietal lobule, and left supramarginal gyrus could be associated with more efficient remapping of tactile signals to the correct spatial locations (Kitazawa S *et al.* 2008) or more efficient associations of tactile stimuli to their external representations (Shore DI *et al.* 2002). In agreement with the idea, Wada M *et al.* (2012), in another fMRI study, found that adapting a crossed hand posture activated the left superior temporal gyrus and the left posterior

parietal areas (specifically the left supramarginal gyrus when the eyes were closed), and the activity of the left posterior parietal areas was associated with the degree of judgment reversal. The same group, in a follow-up study, examined left intraparietal-sulcus-seeded functional connectivity and reported significantly stronger functional connectivity in the right rostral-middle/inferior frontal gyrus and left posterior parietal areas during the crossed posture than during the uncrossed posture (Ora H *et al.* 2016). Therefore, cortical elaboration in the right frontal regions (in addition to the left posterior parietal regions) might improve the process of updating the spatial coordinates of the hands.

On the other hand, the involvement of the left superior and the right middle temporal gyri, which involved so-to-speak biological motion areas, would be better understood by assuming the motion projection hypothesis put forth by Kitazawa and colleagues (Kitazawa S *et al.* 2008; Takahashi T *et al.* 2013; Takahashi T and S Kitazawa 2017). Cortical elaboration (efficiency) of these regions could be associated with a better function in replacing the initial erroneous motion signal with a correct one (Takahashi T *et al.* 2013).

I have so far discussed implications of five of the ten regions (right middle frontal gyrus, right middle temporal gyrus, left superior parietal lobule, left superior temporal gyrus, and left supramarginal gyrus). Of the remaining five regions (the right pars-orbitalis, right and left postcentral gyri, left precuneus, and right cuneus), the left precuneus and the right cuneus were located in the medial part around the parieto-occipital sulcus. Takahashi T and S Kitazawa (2017), by recording MEG signals during crossed-hand tactile TOJ, found that judgment reversal was modulated by the α rhythm of the regions near the parieto-occipital sulcus. They hypothesized that the α rhythm regulates information flow from the superior colliculus, where the anatomical tactile information is represented, to the precuneus by modulating the thalamic nuclei that interconnect

the superior colliculus to the precuneus at 10 Hz. Elaboration of the medial regions might thus contribute to better suppressing the anatomical tactile information coming from the subcortical regions, thereby reducing the chance of inverted judgments.

I finally turn to the postcentral gyrus and the right pars-orbitalis, both of which had a critical power to predict the reversal value but escaped from being identified by the previous imaging studies. I speculate that the activations of these regions in the tactile TOJ task were canceled by a similar amount of activations in the control tasks. As for the involvement of the postcentral gyrus, it is critically important to emphasize that the postcentral gyrus is more than just a simple primary sensory region, and its most caudal part is especially responsible for the integration of bilateral somatosensory, proprioceptive and visual information (Iwamura Y 1998; Borchers S et al. 2011). Therefore, elaboration of the postcentral gyrus might contribute to processing not only somatotopic but also spatial aspects of the tactile stimuli.

The pars-orbitalis is associated with top-down inhibitory control (Chavan CF et al. 2015; Yoo JH et al. 2016). It has been reported that the neural activation and morphological properties of the left and right pars-orbitalis were altered by improvements in a Go/ No-Go task (Chavan CF *et al.* 2015). Moreover, it has been shown that symptom improvement in attention deficit hyperactivity disorder (ADHD) patients through psychological therapy significantly altered the resting-state regional homogeneity (i.e., local connectivity) of the right pars-orbitalis (Yoo JH *et al.* 2016). Thus, a more elaborate and efficient right pars-orbitalis might result in a better top-down control. This fits well with one of the accounts of the crossing effect that integration of external and anatomical spatial representations is regulated by top-down control (Badde S *et al.* 2014; Badde S and T Heed 2016; Badde S *et al.* 2016). Assuming this account, elaboration in the pars-orbitalis would improve a top-down control, so that more weight is put on the external than the

anatomical representations. Moreover, assuming the latest account which put forth that the inverted judgment occurs due to the association of the incorrect hand with the tactile stimulus upon occurrence (Maij F *et al.* 2020), an improved top-down control is beneficial, as it would better inhibit the incorrect hand assignment.

In summary, elaboration of the regions listed in Table 1-1 can possibly improve one's crossed-hand tactile TOJ performance through 1) better integration of the tactile stimuli with the correct spatial representations in the left parietal regions, 2) improvement of motion signals in the motion areas, 3) suppressing the integration of the anatomical tactile signals of the superior colliculus in the precuneus, 4) better representation of spatial information in the postcentral gyrus, or 5) improvement of top-down inhibitory control by the right pars-orbitalis that expels the initial erroneous coupling between a tactile stimulus and the wrong hand. Future studies, designed to test each of these possibilities, would lead to a more comprehensive and elaborate model accounting for the crossing effect of the tactile TOJ task.

Study Funding: This work was supported by KAKENHI (18H0522 and 17H00742) to S.K.

Chapter 2: Brain network during tactile temporal order judgment: a MEG connectivity study

Abstract

Temporal order judgment of two successive tactile stimuli delivered to our hands is often inverted when we cross our hands. The present study aimed to identify the time-frequency profile of the brain network connectivity associated with crossing the hands and making an inverted judgment by using magnetoencephalography. The brain network mainly functioned in the low-alpha band (5~10 Hz) when the hands were uncrossed. However, the network was active in the low-beta band (12~18 Hz) in addition to the low-alpha band when the hands were crossed. In the crossed posture, the participants who had better performance (i.e., less inverted judgments) relied mainly on the low-beta band connectivity. On the other hand, the participants with poor performance strongly utilized both low-alpha and low-beta bands. In conclusion, there are two frequency modes of low-alpha and low-beta connectivity during the tactile temporal order judgment task. Only when the hands are crossed, the brain requires to utilize the low-beta band. Furthermore, superior performance in the crossed posture depends on solely relying on the low-beta and suppressing the low-alpha band. Thus, unlike the low-alpha, the low-beta band should contribute to resolving the confusion in the crossed posture and correctly mapping the touch to the hands.

Introduction

When we are asked to judge the temporal order of two successive tactile stimuli delivered to our hands, we often make inverted judgments when we cross our hands (Yamamoto S and S Kitazawa 2001; Shore DI *et al.* 2002). This phenomenon, known as the crossing effect, indicates that our brain doesn't rely solely on its somatotopic arrangement in perceiving the touch but also takes into account the hand posture (i.e., proprioceptive information). In the last two decades, since the discovery of the phenomenon, various neuroimaging and psychophysiological studies have been conducted to investigate how our brain considers the body posture in the perception of touch and its temporal order, what their neural correlates are, and why we make inverted judgments.

In a functional magnetic resonance imaging (fMRI) study, it has been found that the activation in the left posterior parietal regions was associated with adopting a crossed-hand posture (Wada M *et al.* 2012; Ora H *et al.* 2016). The fMRI study of Takahashi T *et al.* (2013) on the tactile temporal order judgment (TOJ) task has uncovered that the middle temporal gyrus and the parietal (including the supramarginal, superior, and inferior regions), and prefrontal cortex play a major role in the task when the hands are crossed. An fMRI study from another group revealed that the precuneus also plays an important role (Crollen V *et al.* 2017). Likewise, in a magnetoencephalography (MEG) study, it has been reported that the alpha rhythm of the regions near to the medial parieto-occipital sulcus (part of the precuneus and cuneus) modulates our perception of the tactile stimuli in the crossed-hand posture (Takahashi T and S Kitazawa 2017). Furthermore, in my previous structural MRI study, by examining the brain's morphological characteristics and the performance in the crossed-hand tactile TOJ task, I discovered that the pars-orbitalis and postcentral gyrus, in addition to the regions mentioned above, are critical in the task (Moharramipour A and S Kitazawa 2021). They are possibly involved in top-down control and

integration of the somatotopic and spatial postural information, respectively. Previous psychophysiological studies have shown that the performance in the crossed-hand TOJ task is regulated by top-down control (Badde S *et al.* 2014, 2016). Last, it is noteworthy that evidence from the usage of visual distractors (Shibuya S et al. 2007) and comparing the performance of congenitally blind and sighted people (Röder B et al. 2004; Crollen V *et al.* 2017) have shown that, in general, the visual pathway, including the occipital and parietal lobe, should be important in how we perceive the tactile spatial information. Despite all the discoveries, there is still not much known about the time-frequency dynamics of the brain regions' interactions during the task.

In the present study, by recording the MEG signals, I aimed to examine how the interactions between the above-mentioned regions alter during the tactile TOJ task when the hands are crossed and uncrossed and when the judgment is inverted and correct. As far as I know, there are only two electrophysiological studies done on the tactile TOJ task (Soto-Faraco S and E Azañón 2013; Takahashi T and S Kitazawa 2017), and none of them have investigated the interactions across time and frequency between the regions. The high temporal resolution of the MEG electrophysiological signals makes it suitable for extracting the interactions (i.e., connectivity) (Moharramipour A et al. 2018; He B et al. 2019; Mostame P et al. 2019). The connectivity analysis can provide more detailed information about brain function than the conventional activation-detection approach (Bullmore E and O Sporns 2009; Sporns O 2010). Here, I identified how the posture of the hands affects the brain network function, how the network of the people with superior or poor performance is different, and what in the network contributes to making a correct and inverted judgment.

Methods

Participants

Twenty-eight right-handed volunteers, ranging in age between 20 to 49 years old, participated in the present study. All participants were neurologically normal, and written informed consent was obtained from them before the experiment. The study was approved by the Ethical Review Board of Osaka University, Graduate School of Frontier Biosciences.

Experiment

One-hundred-and-sixty-channel whole-head MEG data (PQA-160C, Yokogawa Electric, 1 kHz sampling) were acquired from the participants while performing the tactile TOJ task. Figure 2-1 schematically shows the experimental paradigm used in the present study. Participants voluntarily started each trial by resting their index fingers on a photosensor. After a random delay (1800~2800 ms), two successive tactile stimuli with stimulus onset asynchrony (SOA) of 100 ms were delivered to the tip of each ring finger. Two isolated current stimulators (SEM-4201, Nihon Koden) were used to deliver the tactile stimuli (square current pulses lasting for 0.1 ms at twice the threshold intensity). Participants were instructed to judge which hand was stimulated second. They needed to wait for 1000~1500 ms to receive a visual cue (blue dot) and then overtly respond by raising the index finger of the hand they judged as being stimulated second. They were instructed to fixate on a red dot without blinking until they give their response. The experiment was conducted in the crossed- and uncrossed-hand postures in fifteen participants, and in the crossed posture alone in the remaining thirteen participants. During the experiment, participants were in a supine position with their heads inside the MEG scanner. Some of the data were borrowed from those used in (Takahashi T and S Kitazawa 2017).

To prevent premature judgment after receiving the first tactile stimulus, in some trials, the two stimuli were delivered to the same hand (catch trials). Three types of trials, right- then left-hand (RL) stimulation, left- then right-hand (LR) stimulation, and catch trials, were randomly used in the experiment. Fifteen of the participants completed the experiment both in the crossed- and uncrossed-hand postures. For them, two sessions were conducted in the crossed posture and one session in the uncrossed posture, and each session consisted of 90 LR, 90 RL, and 20 catch trials. The rest (thirteen) of the participants completed the experiment in only the crossed posture. They participated in two sessions, and each session had 50 RL, 50 LR, and 100 catch trials.

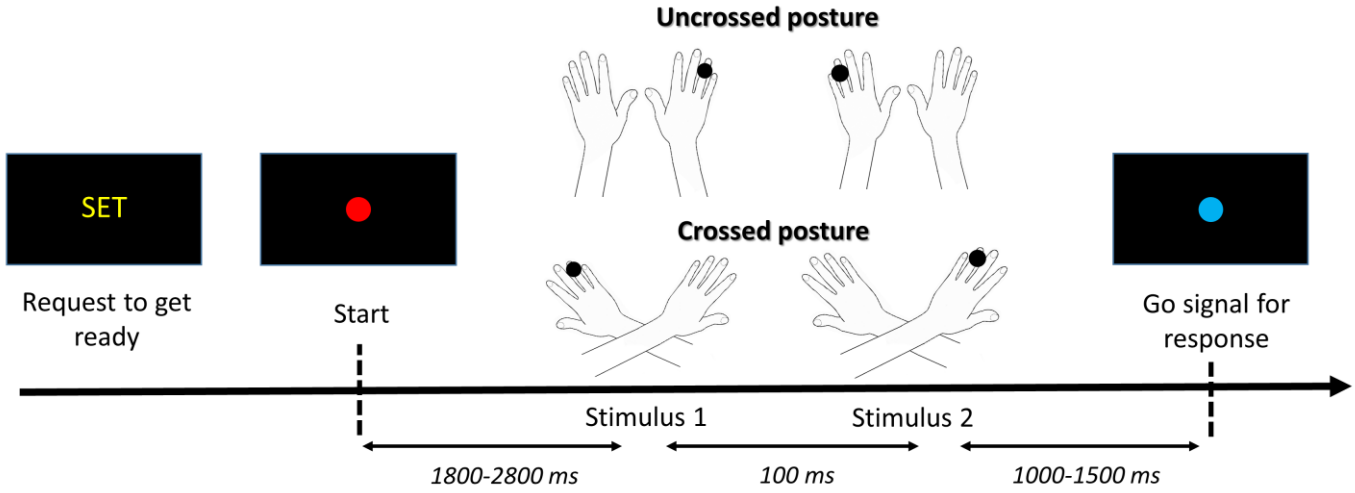

Fig. 2-1. Schematic of the experimental paradigm. Participants judged the order of two successive tactile stimuli delivered to each hand. They were instructed to fixate on a red dot and respond by raising the index finger of the hand they judged as being stimulated second. They gave their response immediately after receiving a blue dot go sign.

T1-weighted structural MRI image of each participant was acquired by using 3D-SPGR sequence on a 3-tesla whole-body scanner (Discovery MR750w GEM, repetition time (TR) = 9.1 ms, echo time (TE) = 2.7 ms, flip angle (FA) = 15 degrees, field of view (FOV) = 240×240 mm, and resolution = 1×1×1 mm).

Analysis

Preprocessing. MEG data were epoched with respect to the onset time of the first tactile stimulus, downsampled to 200 Hz, and filtered (high passed, and band stopped 60 Hz and its harmonics). Independent component analysis (ICA) was applied to remove the electrocardiogram (ECG) artifact. Furthermore, I examined the signals of each trial, visually and statistically (e.g., variance, range, and z-value), and removed the bad/outlier ones. It is noteworthy that the preprocessed trials consisted of two categories of crossed and uncrossed postures and subcategories of RL and LR with two subclasses of inverted and correct judgment.

Inverse problem. Brain sources on MNI space were localized on individual structural MRI images by applying the inverse of the deformation field, which normalizes the structural MRI to MNI space. The coordinate system of the MRI image and the positions of the MEG sensors were linked by three fiducial points (Nasion, left and right pre-auricular points), and then the lead-filed matrix was estimated based on the single-shell model (Nolte G 2003).

The relation between the brain sources and the MEG sensors in the Bayesian framework is as follows (Belardinelli P et al. 2012; López JD et al. 2014):

$$\mathrm{Y} = \mathrm{LJ} + \varepsilon \tag{2-1}$$

where $\mathrm{Y} \epsilon \mathbb{R}^{N_s \times N_n}$ is the sensor space matrix formed by N_s sensors and N_n time samples, $\mathrm{L} \epsilon \mathbb{R}^{N_s \times N_q}$ is the lead-field matrix, $\mathrm{J} \in \mathbb{R}^{N_q \times N_n}$ is the activity matrix of N_q sources, and ε is a zero-mean Gaussian noise with the covariance of Q_ε. By assuming a zero-mean Gaussian process for the sources ($p(J) \sim \mathcal{N}(0, \mathrm{Q})$), the solution of Eq. (2-1) in the Bayesian framework is as follows (López JD *et al.* 2014):

$$\hat{J} = \mathrm{QL}^T (Q_\varepsilon + LQL^T)^{-1} Y \tag{2-2}$$

where Q is the covariance matrix of the source vector.

Certain prior structures with unknown hyper-parameters were assumed for the covariance matrices of Q and Q_ε. Those hyper-parameters were estimated by the restricted maximum likelihood (ReML) approach and having the free energy as the objective function (Friston K et al. 2008). The prior assumption for Q_ε was as follows:

$$Q_\varepsilon = h_0 I_{N_s} \tag{2-3}$$

where h_0 is a hyper-parameter and I_{N_s} is a N_s dimensional identity matrix. The prior for the Q was assigned based on the empirical bayesian beamformer (EBB) method (Barnes GR and A Hillebrand 2003):

$$\begin{aligned} &{\delta_q}^2 = ({L_q}^T {\Sigma_y}^{-1} L_q)^{-1},\ \Sigma_y = E(YY^T),\ q = 1, \cdots, N_q \\ &\mathrm{Q} = h_1 \mathrm{diag}({\delta_q}^2) \end{aligned} \tag{2-4}$$

$L_q \epsilon \mathbb{R}^{N_s \times 1}$ is the q[th] column of the lead-field matrix (L), $\Sigma_y \epsilon \mathbb{R}^{N_s \times N_s}$ is the sensors' covariance matrix, and h_1 is a hyper-parameter. In the EBB method, the prior is estimated from the data, and the sources are assumed to be independent. It has been reported that for data having a moderate signal-to-noise ratio, the EBB prior provides better accuracy than other common priors in the Bayesian framework (e.g., multiple sparse prior, minimum norm model, and etc.) (Belardinelli P *et al.* 2012).

It is noteworthy that I used a reduced sensor space ($\tilde{L}\ \epsilon \mathbb{R}^{N_{\acute{s}} \times N_q}, \tilde{Y}\ \epsilon \mathbb{R}^{N_{\acute{s}} \times N_n}$) in all analyses mentioned above. Sensor space was reduced to $N_{\acute{s}}$ dimensions by applying singular value decomposition (SVD) over the lead-field matrix and removing its small eigenvalues. This will help removing spatial noises and also reducing computational costs (Belardinelli P *et al.* 2012).

I limited the solution of the inverse model to eighteen sources (Fig. 2-2A, Table 2-1). The sources were placed on the center of the anatomical regions found in my previous morphological MRI study playing a crucial role in the tactile TOJ task (Moharramipour A and S Kitazawa 2021).

Those regions have been reported in different functional neuroimaging studies of the tactile TOJ as well (Wada M *et al.* 2012; Takahashi T *et al.* 2013; Ora H *et al.* 2016; Crollen V *et al.* 2017; Takahashi T and S Kitazawa 2017). It is worth noting that applying our previous knowledge by restricting the inverse solution to specific brain regions will simplify the model, and at the same time, it might even result in a more accurate model fitting.

All the analyses above (i.e., calculation of the lead-field matrix and the inverse model) were implemented by using the SPM 12 (version 7219) toolbox (Penny WD et al. 2011).

Brain areas (Sources)	Left hemisphere MNI coordinate			Right hemisphere MNI coordinate		
	x	y	z	x	y	z
Postcentral gyrus	-48	-21	41	47	-21	40
Supramarginal gyrus	-55	-34	31	54	-33	31
Superior parietal lobule	-23	-65	50	22	-65	52
Precuneus	-10	-59	37	9	-58	36
Superior temporal gyrus	-55	-9	-6	56	-7	-7
Middle temporal gyrus	-60	-22	-15	59	-24	-17
Cuneus	-6	-77	20	9	-79	21
Pars-orbitalis	-46	35	-14	46	35	-15
Middle frontal gyrus	-35	48	14	34	49	12

Table 2-1. MNI coordinates of the eighteen brain sources used in the functional connectivity analysis (Fig. 2-2A).

Functional connectivity analysis. In the present study, a functional connectivity method called debiased weighted phase lag index (dWPLI) was implemented (Vinck M et al. 2011). The dWPLI measures the non-directional coupling between two regions across time and frequency as follows:

$$S_{ij}(f,t) = x_i(f,t)x_j{}^*(f,t)$$

$$dWPLI_{ij}(f,t) = \left|\frac{\sum_{m=1}^{N}\sum_{n\neq m}\zeta\,(S_{ij}(f,t)_m)\zeta\,(S_{ij}(f,t)_n)}{\sum_{m=1}^{N}\sum_{n\neq m}\left|\zeta\,(S_{ij}(f,t)_m)\zeta\,(S_{ij}(f,t)_n)\right|}\right| \quad (2\text{-}5)$$

Where f and t are frequency and time, x_i and x_j are the time-frequency transform of the signals of i^{th} and j^{th} regions in one trial, S_{ij} is their cross-spectrum, N is the number of trials, and ζ indicates the imaginary part of the complex value. Simply put, if there is a meaningful consistent phase lag between two signals across trials, it means that they are coupled. The stronger the coupling is, the dWPLI value goes higher, above zero, up to one. I calculated the dWPLI over the frequency from 5 to 30 Hz (every 1 Hz) and the time from -1 to 1.5 s (every 40 ms), for each of 153 ($\frac{18\times17}{2}$) pairs across the 18 regions of interest (e.g., Fig. 2-2C). 0 s corresponds to the onset time of the first tactile stimulus. In the calculation of the time-frequency transform, I used a multi-taper convolution method with a time window of 400 ms. It is noteworthy that in representing the time-frequency profile of connectivity, I set the 75th percentile of the window as a time-point rather than its center (50th percentile). This was solely done to have a better visualization around the onset time.

The reason that I chose dWPLI is that, firstly, it is insensitive to volume conduction. The volume conduction can result in fallacious detection of coupling between two signals that are not coupled, but both are just a reflection of another third signal. The volume conduction profoundly exists in the electrophysiological signals recorded by EEG or MEG. Secondly, it is insensitive to sample size bias. This is extremely important in the present study since the number of trials is not the same in different conditions (e.g., between the crossed and uncrossed postures). Vinck M *et al.*

(2011) have shown that in the dWPLI, for the number of trials (N) above 30, the effect of sample size bias is small (i.e., its value doesn't change noticeably with the increase of N).

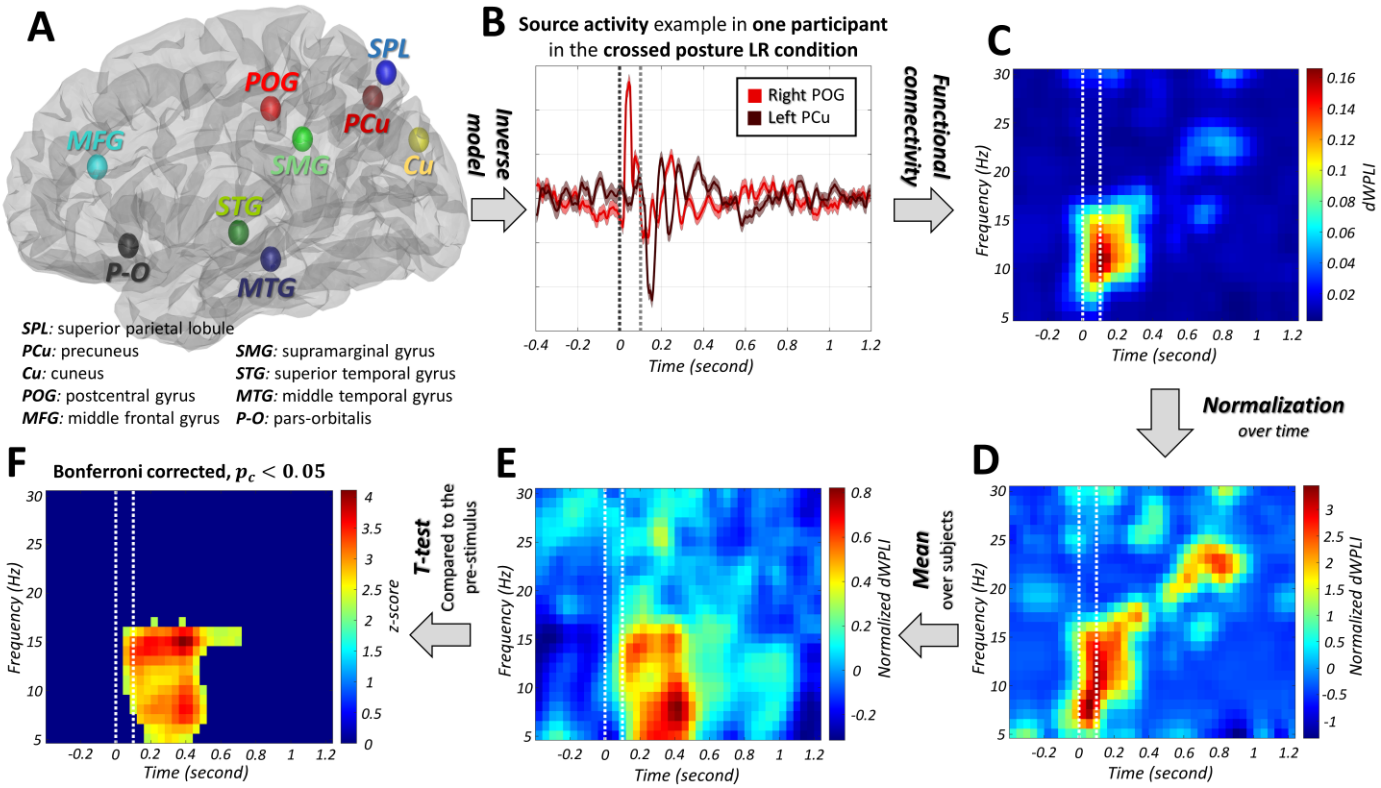

Fig. 2-2. Summary of the source-level functional connectivity analysis. (A) Brain sources in the regions that have previously been shown to play a major role in the tactile TOJ task (Table 2-1). (B) Source activity of the left precuneus and right postcentral gyrus estimated by the EBB inverse model in the crossed posture LR condition in one example participant. Solid lines and shaded areas represent the mean and standard error across trials, respectively. Dotted lines show the delivery of the first (left-hand) and second (right-hand) tactile stimuli. (C) Time-frequency dWPLI calculated between the source activity example of B. (D) Normalization applied on the dWPLI of C at each frequency. (E) The normalized dWPLI between the left precuneus and right postcentral gyrus averaged across the subjects in the crossed posture LR condition. (F) The z-score of the paired-sample t-test calculated between the post- and pre-stimulus of E that passed the non-parametric permutation test ($p_c < 0.05$, Bonferroni corrected) (Fig. 2-3).

The goal is to see the evolution of coupling between the brain sources during the task. Therefore, I normalized the dWPLI over time for each frequency row (Fig. 2-2D). This enables detecting at what time and between which regions there was a meaningful increase or decrease in

the strength of coupling across the group of subjects. Figure 2-2E shows an example of the normalized dWPLI at each time-frequency bin averaged across the participants.

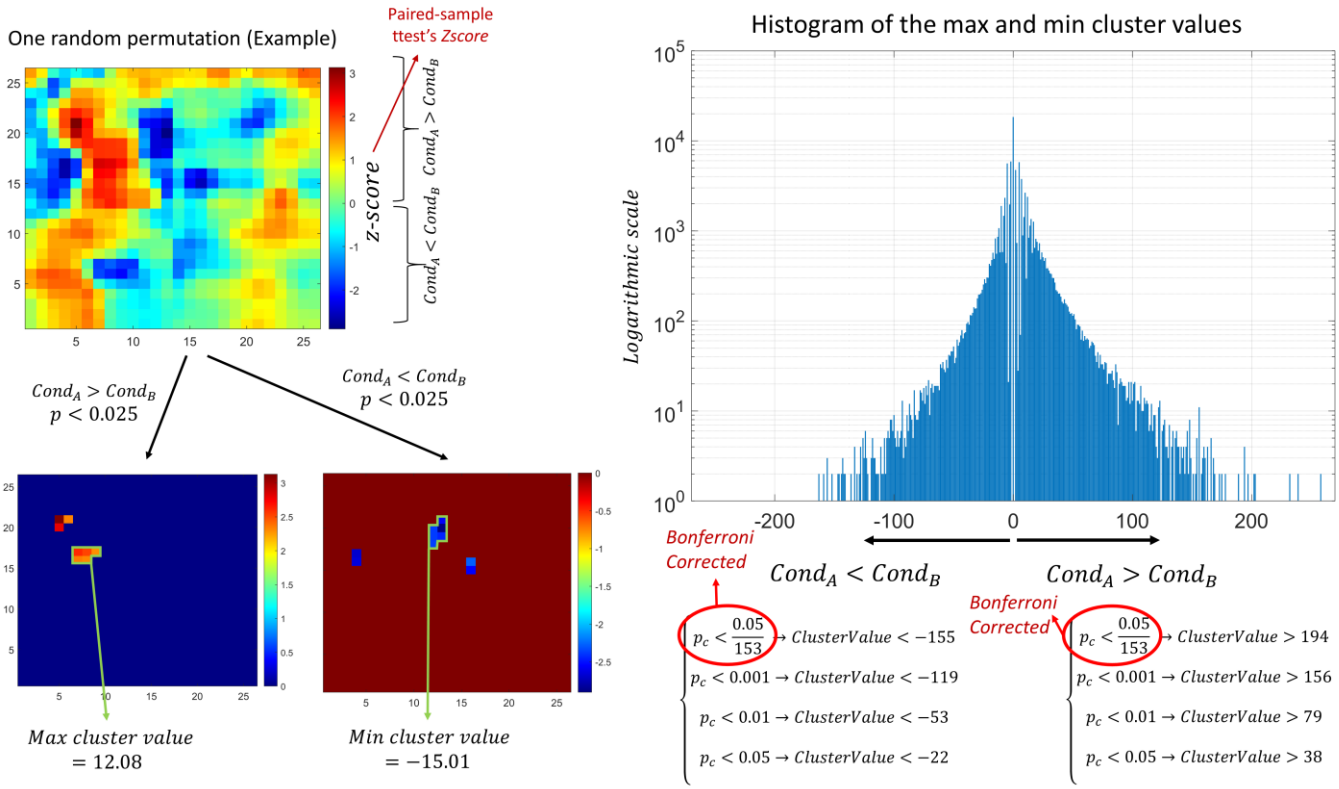

Fig. 2-3. Summary of the non-parametric permutation statistical test. Top left panel shows an example of the *z*-score of the paired-sample t-test calculated between the pre- and post-stimulus for a permutation dataset. In a permutation dataset, the post- and pre-stimulus periods of the subjects were randomly permutated. Bottom left panels show the *z*-scores that corresponded to a *p*-value smaller than the critical threshold of 0.025. The clusters with maximum positive and negative accumulated *z*-scores were extracted. Top right panel shows the histogram of the maximum *z*-scores extracted from a large number of permutation datasets. This histogram represents the null hypothesis in which there should be no time-frequency cluster significantly different between the post- and pre-stimulus. The significant cluster's *z*-score was shown for alpha thresholds (p_c) smaller than 0.05/153 (Bonferroni correction), 0.001, 0.01, and 0.05 in both tails of the histogram.

To derive the brain network (couplings) that emerged after the delivery of the tactile stimulus ($0s$), I applied a paired-sample t-test between the post- and pre-stimulus' normalized dWPLI. At each frequency row of the normalized dWPLI, its median value associated with the time bins of

the pre-stimulus ($-1\ s$ to $0\ s$) was calculated. Then at each frequency, a paired-sample t-test was applied on the group of subjects between each of their time bins ($-1\ s$ to $1.5\ s$) and their pre-stimulus' median value. By doing so, we were able to find the couplings significantly strengthened or weakened compared to the pre-stimulus across the time and frequency (Fig. 2-2F).

After applying the paired-sample t-test, to identify the cluster size of significance in time and frequency, I used a non-parametric permutation test (Maris E and R Oostenveld 2007). The pre- and post-stimulus windows of the subjects were randomly permutated, and the z-score and *p*-value of the paired-sample t-test were calculated. Then the clusters with a *p*-value smaller than the critical threshold of 0.025 were extracted. The cluster with the maximum positive and negative accumulated z-score was identified. This process was repeated a large number of times, and the histogram of the maximum cluster values was acquired (Fig. 2-3). This histogram corresponds to the null hypothesis in which there should be no time-frequency cluster significantly different between the pre- and post-stimulus. Finally, the threshold for a significant cluster value was determined by using this histogram and a specified alpha threshold (p_c) (i.e., probability of falsely detecting a cluster as significant). Moreover, I accounted for the multiple comparisons by applying the Bonferroni correction. In this correction, since there are 153 connectivity pairs, the alpha threshold needs to be divided by 153. The alpha thresholds of $0.05/153$ (Bonferroni correction), 0.001, 0.01, and 0.05 were employed in the present study.

I applied the analysis and the statistical test on the crossed posture's RL and LR (twenty-eight subjects), and the uncrossed posture's RL and LR conditions (fifteen subjects). Furthermore, I divided the subjects into two groups of the reversers, the ones who had poor performance (i.e., had a considerable number of inverted judgments) in the crossed condition (sixteen subjects), and the non-reversers, the ones who had a good performance (twelve subjects). I applied the analysis

separately on these two groups to compare their brain networks. In addition, as there were enough inverted trials in the reverses LR condition, I could robustly extract their network associated with their inverted judgments. So, I separately derived the networks for correct and inverted judgments just in the reversers and in their LR condition.

In choosing the reversers and non-reversers, I looked at the ratio of their inverted judgments (reversal) in the crossed posture and in its each RL and LR conditions. The reversers had the reversal of 20~63% (36±11%) with 21~77 % (47±18%) in the LR, and 2~52% (26±16%) in the RL condition. On the other hand, the non-reversers had the reversal of 1~23% (12±7%) with 1~28% (11±8%) in the LR, and 1~31% (13±10%) in the RL condition.

Results

In all the experimental conditions, the brain network connectivity was increased after the stimulus onset. There were just a few and negligible (not statistically impressive) number of connections weakened after the stimulus onset. So, in studying the experimental conditions, I focused on the brain networks that were significantly stronger in post- than pre-stimulus (positive network). Figure 2-4 shows the time-frequency profile of the positive brain network associated with the crossed and uncrossed postures in the LR condition. Figure 2-5 shows the same for the RL condition. In the crossed posture, the network mainly functioned in the low-beta frequency band (12~18 Hz), with its peak at around 15 Hz. The network was active in the lower frequencies, like the low-alpha band (5~10 Hz); however, it got denser in the low-beta band. In other words, most of the connections were functioning in the alpha and the low-beta band, and some other connections only in the low-beta band (Figs. 2-4B and 2-5B). On the contrary, in the uncrossed posture, the main activity of the brain network was in the low-alpha band, with its peak at around 6 Hz. Most of the connections were channeled to the low-alpha band and didn't continue functioning in the higher frequencies (Figs. 2-4D and 2-5D). Up to 700ms after the stimulus onset, the low-beta band connectivity density of the network was significantly higher in crossed than uncrossed posture (Figs. 2-4F and 2-5F). In short, there were two modes of connectivity across the frequency, the low-alpha and the low-beta modes. Brain functioned only on the low-alpha mode when the hands were uncrossed; however, it used both modes, even more profoundly the low-beta mode, when the hands were crossed.

Furthermore, in the uncrossed posture, especially in the LR condition, a great degree of lateralization could be observed in the network. There was a great ratio of intra-hemispheric connections in just one of the hemispheres (Figs. 2-4C and 2-5C). This lateralization was on the

hemisphere that received the first tactile stimulus, the right hemisphere in the LR, and the left hemisphere in the RL condition. On the other hand, in the crossed posture, a smaller degree of lateralization existed in the network. There was a higher ratio of the inter-hemispheric connections than the intra-hemispheric connections (Figs. 2-4A and 2-5A). In both the crossed and uncrossed conditions, the rise in the left and right intra-hemispheric connections coincided with the order of the tactile stimuli (i.e., left then right hemisphere in the RL, and vice versa in the LR condition). Furthermore, it is noteworthy that the activity duration of the brain network was slightly longer in the crossed than the uncrossed posture.

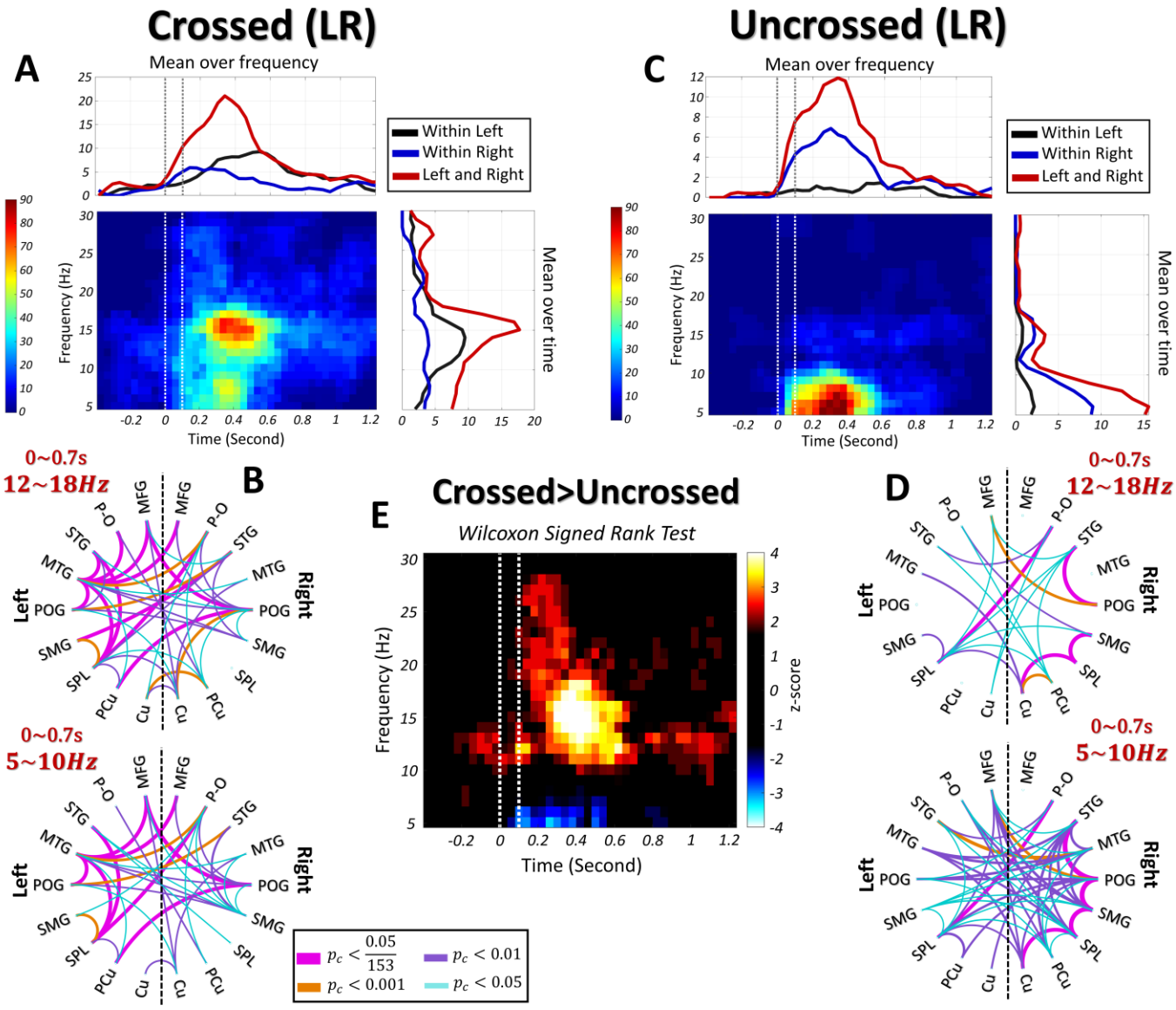

Fig. 2-4. Result of the source-level functional connectivity analysis (the connectivity that was significantly stronger in post- than pre-stimulus) in the LR condition. Accumulation of the z-scores of all 153 region pairs that passed the statistical test (Figs. 2-2F and 2-3) with $p_c < 0.05$ is shown for the (A) crossed and (C) uncrossed postures. The top subplot shows the average of the color map across frequency, and the right subplot shows its average across time. The value related to the inter-hemispheric connections (i.e., the connections between the left and right hemisphere, 81 pairs) is shown with the red color, and the value related to the intra-hemispheric connections (i.e., the connections within a hemisphere, 36 pairs) is shown with the black and blue colors for the left and right hemispheres, respectively. Time 0s corresponds to the delivery of the first tactile stimulus (i.e., the left-hand stimulus). The brain networks associated with the time window of 0 to 700ms and the frequency range of 12 to 18 Hz (low beta band) and 5 to 10 Hz (low alpha band) are shown for the (B) crossed and (D) uncrossed postures. The magenta, orange, purple, and light blue colors indicate the connections that passed the statistical test with a p_c smaller than 0.05/153 (Bonferroni correction), 0.001, 0.01, and 0.05, respectively. A lower p_c correspond to a significant and larger time-frequency cluster of connectivity. MTG: middle temporal gyrus, STG: superior temporal gyrus, SPL: superior parietal lobule, SPM: supramarginal gyrus, POG: postcentral gyrus, P-O: pars-orbitalis, MFG: middle frontal gyrus, Cu: cuneus, PCu: precuneus. (E) z-score of the Wilcoxon signed-rank test calculated between the color maps in A and C. It represents the network's density difference between the crossed and uncrossed postures across time and frequency. Warm and cool colors indicate crossed > uncrossed and crossed < uncrossed, respectively.

Figures 2-6 and 2-7 show the positive network of the reversers and non-reversers in the crossed posture LR and RL conditions, respectively. The brain network of the non-reversers mainly functioned in the low-beta band, with its peak at 15 Hz. However, the reversers' network was strongly active in both low-alpha and low-beta modes. The network density in the low-alpha band was significantly higher in the reversers than non-reversers (Figs. 2-6F and 2-7F). As reversers had poor performance (i.e., a high number of inverted judgments), it suggests that using the low-alpha mode should negatively affect perceiving the tactile stimuli and their temporal order when the hands are crossed.

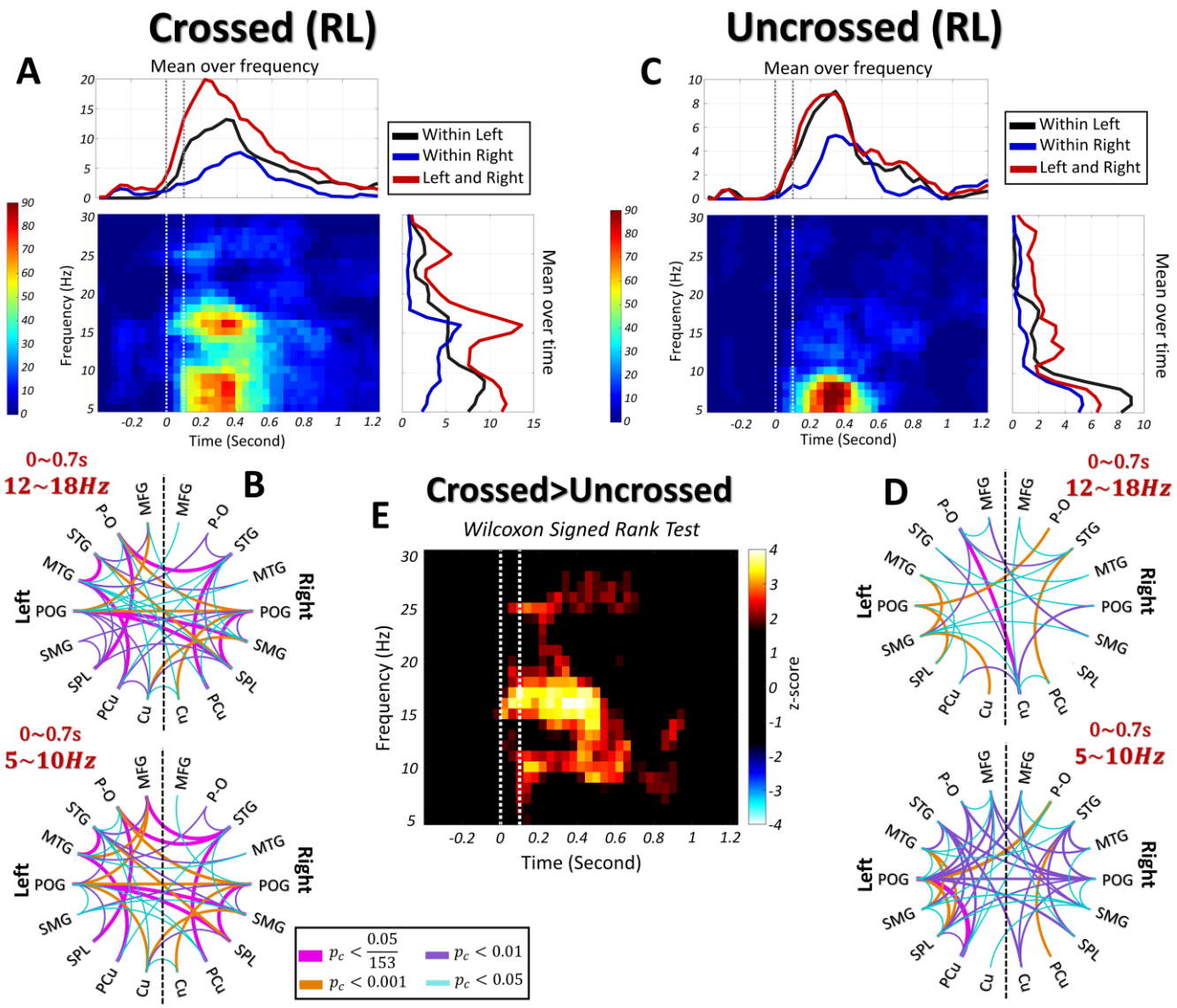

Fig. 2-5. Result of the source-level functional connectivity analysis (the connectivity that was significantly stronger in post- than pre-stimulus) in the RL condition. The remaining descriptions of the figure are the same as those in Fig. 2-4.

In Figure 2-8, I showed the positive network of the reversers when they made correct and inverted judgments in the crossed posture LR condition. Their network activity started earlier and lasted longer when they made correct judgments. The early phase started with the onset and lasted for 300 ms, and it was in the high alpha and low-beta band (Fig. 2-8A, number 1). The later phase was in the alpha and low-beta band and started around 500 ms after the onset (Fig. 2-8A, number

3). The later phase was more lateralized to the left hemisphere and got denser connectivity in the left superior partial lobule and middle temporal gyrus. When they made inverted judgments, these two phases of connectivity were missing (Fig. 2-8F). Furthermore, there was a lack of connectivity in the posterior parts of the brain (i.e., cuneus, precuneus, superior parietal lobule, and supramarginal gyrus), especially in the low-alpha band (Fig. 2-8D). This may imply that those regions should play a major role in making a correct judgment when the hands are crossed.

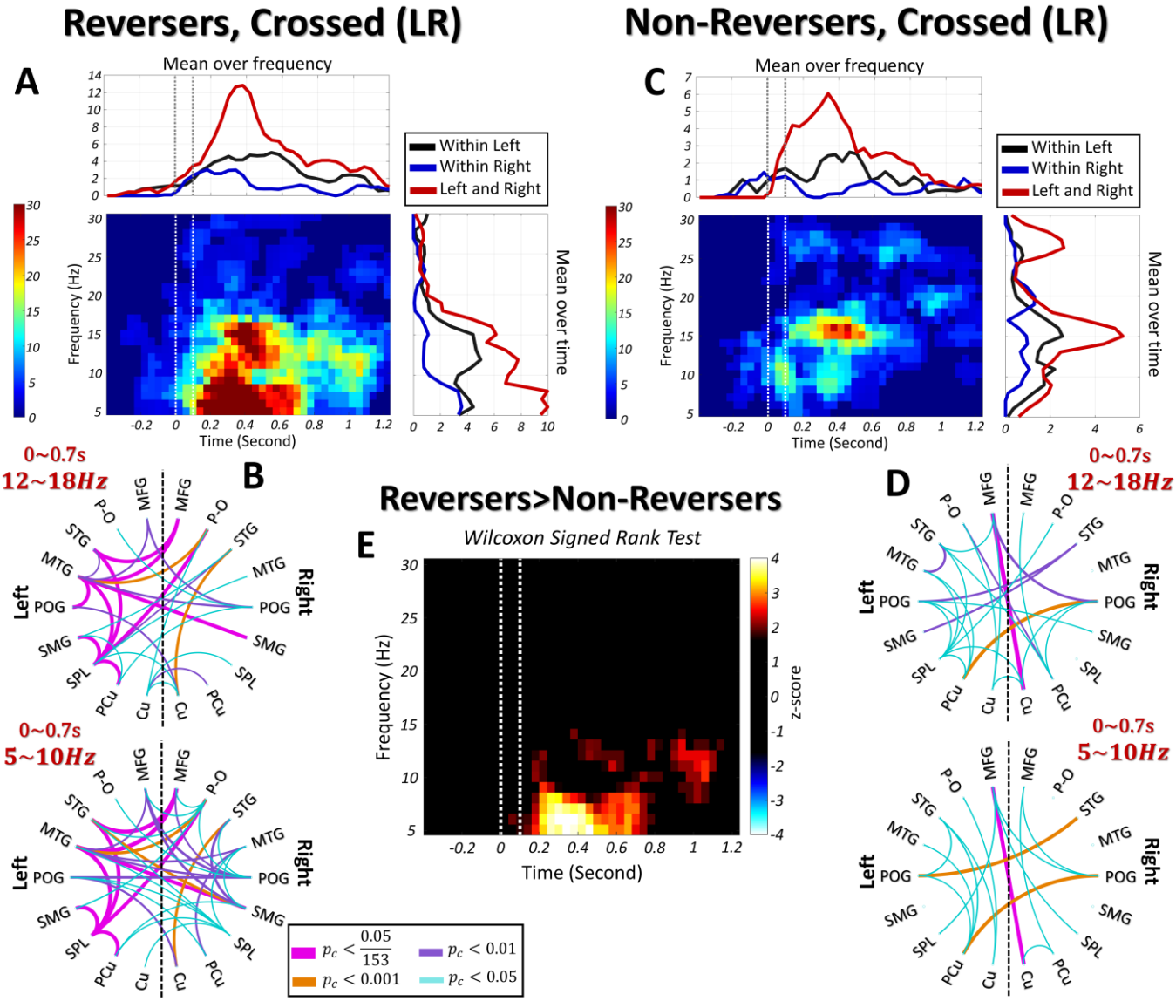

Fig. 2-6. Connectivity profile of the LR crossed-hand condition in the (A, B) reversers (participants with considerable inverted judgments) and (C, D) nonreversers (participants with few inverted judgments).

Further descriptions of the figure are similar to those in Fig. 2-4. (E) z score of the Wilcoxon signed-rank test calculated between the color maps in A and C. It represents the network's density difference between the reversers and nonreversers. Warm and cool colors indicate reversers > nonreversers and reversers < nonreversers, respectively.

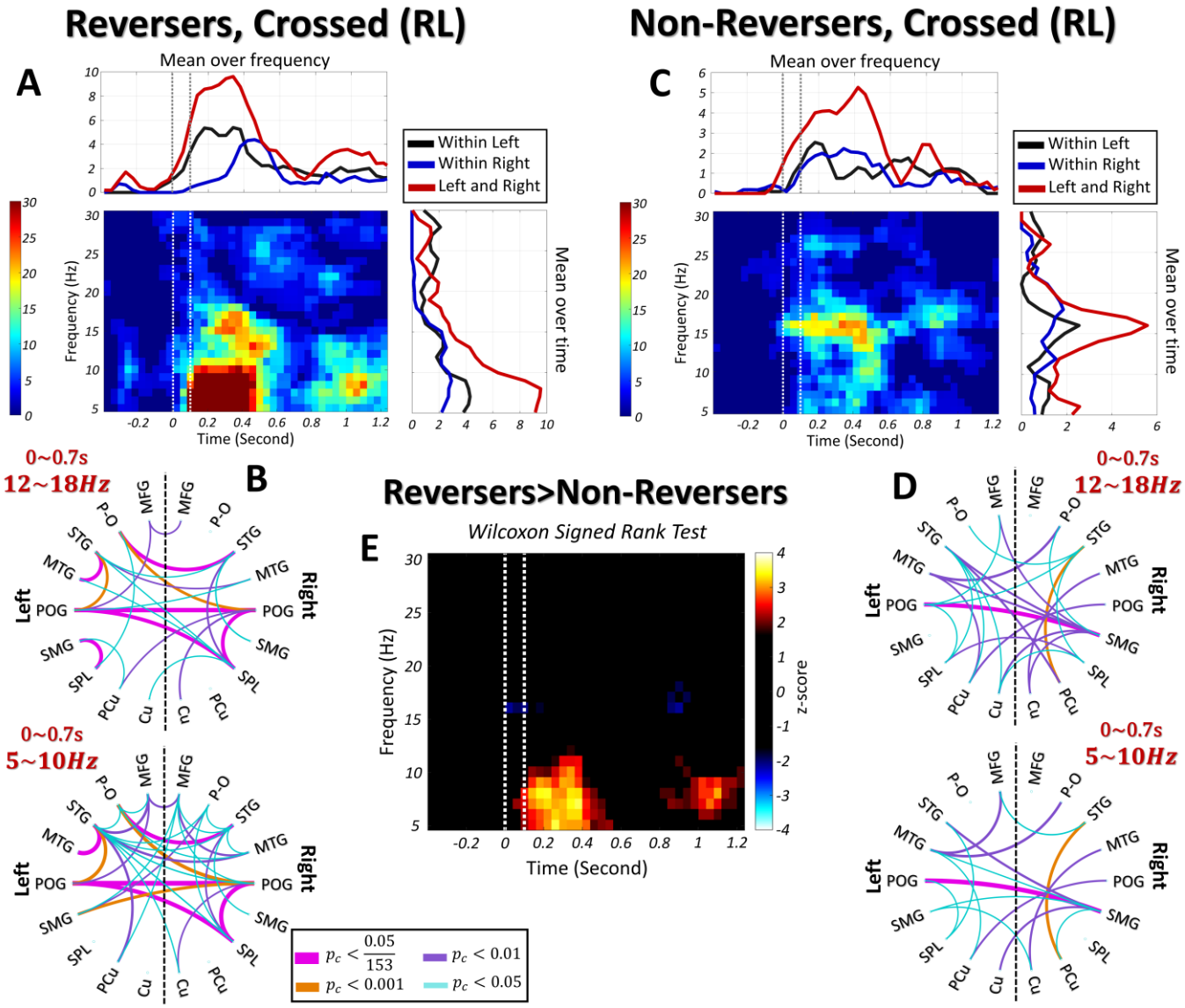

Fig. 2-7. Connectivity profile of the RL crossed-hand condition in the reversers and nonreversers. The remaining descriptions of the figure are the same as those in Fig. 2-6.

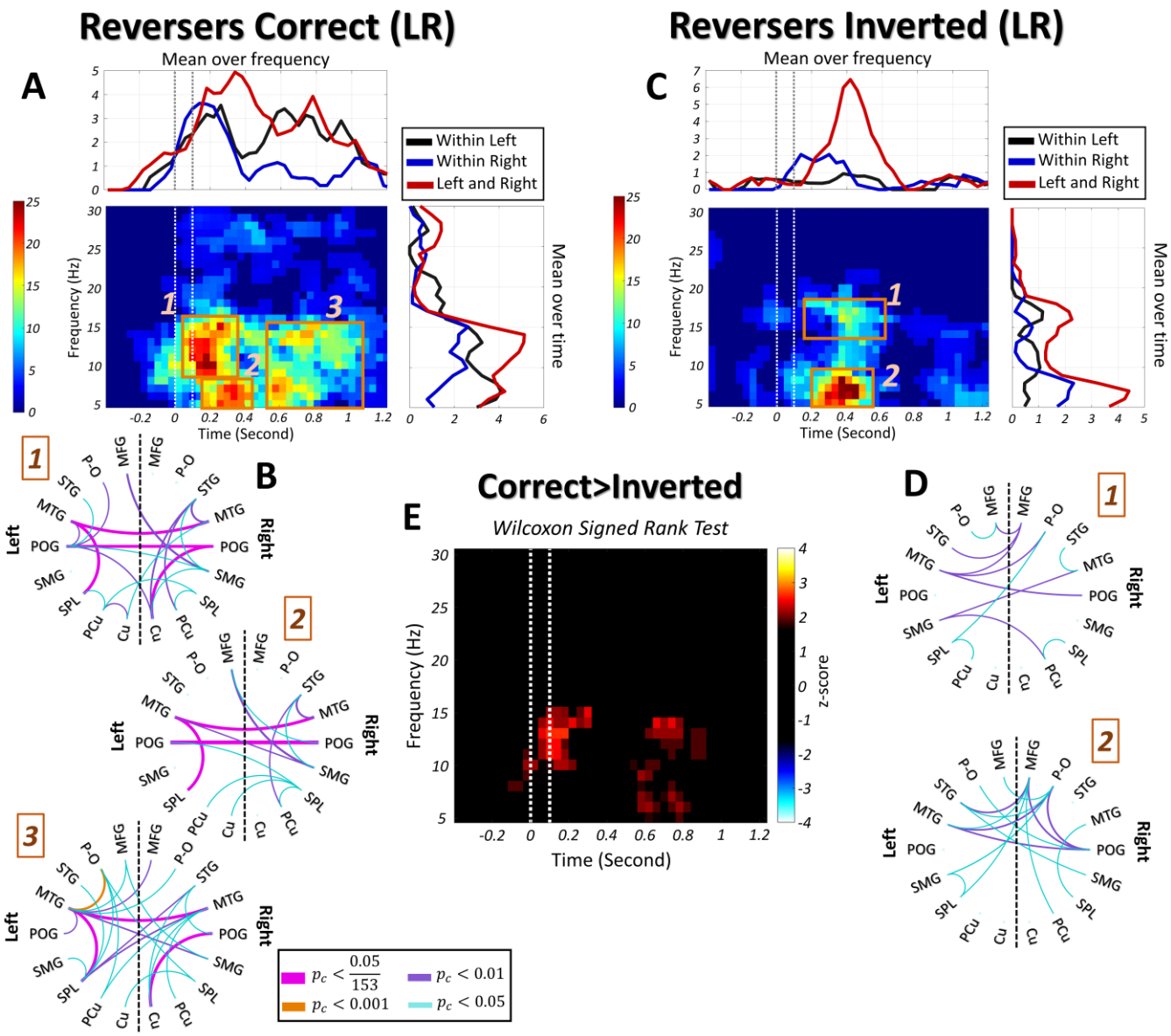

Fig. 2-8. Connectivity profile of the LR crossed-hand condition in the reversers when they made (A, B) correct and (C, D) inverted judgments. (B) and (D) show the brain networks associated with the major hubs of the time–frequency maps of A and C, respectively. The other detailed descriptions of the figure are similar to those in Fig. 2-4. (E) z score of the Wilcoxon signed-rank test calculated between the color maps in A and C. It represents the network's density difference between when the reversers made a correct and inverted judgment. Warm and cool colors indicate correct > inverted and correct < inverted, respectively.

Discussion

The brain network was less lateralized, had a greater ratio of inter-hemispheric connections, and was longer activated in the crossed than uncrossed posture. Moreover, its activity extended to a higher frequency band. In the uncrossed posture, the network mainly utilized the low-alpha band; however, it used the low-alpha and the low-beta band (more profoundly the low-beta band) in the crossed posture. These observations should correspond to the fact that the crossed posture is more difficult and thus, requires more processing power. Similarly, it has been reported that an increase in task difficulty in a bimanual coordination task was associated with a higher beta band power and greater inter-hemispheric connections (Rueda-Delgado LM et al. 2017). The beta band oscillation is implicated in attentional processes (Gross J et al. 2004; Wróbel A et al. 2007), and high-level cognitive functions, like solving creative problems (divergent thinking) (Razumnikova OM 2004). Moreover, better performance in the attentional tasks (Gross J *et al.* 2004; Gola M et al. 2013) or the divergent thinking task (Razumnikova OM 2004) was associated with higher beta-band activity. Therefore, a stronger beta-band activity should reflect a higher state of attention and sensitivity to stimuli. Perceiving touch when the hands are crossed is far more complex than when they are not crossed (Heed T and E Azanon 2014), so it requires a high state of attention and vigilance. That might be why the brain channeled its connectivity to the low-beta band in the crossed but not uncrossed posture.

Furthermore, I discovered that the non-reversers (the participants with a superior performance) utilized the low-beta band connectivity more than the low-alpha band connectivity. On the other hand, the reversers (the participants with poorer performance) relied heavily on the low-alpha band connectivity and didn't suppress its network. Therefore, I speculate that the low-alpha network should probability contain incorrect information about the spatial location of the

stimuli. In other words, it functions based on the anatomical frame, which is a naïve representation of the stimuli just based on the somatosensory information (Badde S *et al.* 2014; Badde S and T Heed 2016; Badde S *et al.* 2016; Maij F et al. 2020). However, the low-beta network should likely contain the correct spatial locations generated by integrating somatosensory and spatial postural information (i.e., external frame). That might also explain why the brain utilized only the low-alpha connectivity when the hands were uncrossed. Since, in the uncrossed posture, correct judgments can be made just from the anatomical frame.

When the reversers made an inverted judgment, lack of connectivity was observed in the posterior regions of the brain, including the cuneus, precuneus, superior parietal lobule, and supramarginal gyrus. The sources of the precuneus and cuneus were located anterior and posterior to the parieto-occipital sulcus. It has been reported that the parieto-occipital sulcus is one of the main regions involved in reaching tasks, explicitly planning to point at a target (De Jong B et al. 2001; Connolly JD et al. 2003). Furthermore, legion on the parieto-occipital sulcus and superior parietal lobule was associated with the inability to visually guide an arm movement (optic ataxia) (Karnath H-O and M-T Perenin 2005). In non-visual (postural) reaching tasks as well, the superior parietal lobule and precuneus play a significant role (Pellijeff A et al. 2006). They are important in maintaining and updating the limbs' spatial position. Neuronal recording from the superior parietal lobule (area 5) of monkeys has also shown that this region is sensitive to the limbs' spatial position (limbs crossed the body midline) (Graziano MS et al. 2000). Similarly, in an fMRI study, it has been reported that crossing of the hands, specifically the left hand, activated the superior parietal lobule (Lloyd DM et al. 2003). The supramarginal gyrus is also shown to play a significant role in the hands' proprioception-related functions (Ben-Shabat E *et al.* 2015; Findlater SE *et al.* 2018). Thus, overall, these posterior regions (i.e., cuneus, precuneus, superior parietal lobule, and

supramarginal gyrus) should play a major role in awareness of the hand posture and subsequently mapping the tactile stimuli to the hands in space.

Last, I observed that when the reversers succeeded in making a correct judgment, the activity of their network contained an early and late phase of function (Fig. 2-8A, numbers 1 and 3). Previous psychophysiological studies have shown that when we cross our hands, our brain initially perceives a touch on the wrong hand and then maps it to the correct hand (Groh JM and DL Sparks 1996; Azañón E and S Soto-Faraco 2008; Overvliet KE *et al.* 2011). Therefore, I hypothesize that these two phases might correspond to an early start in suppressing the initial erroneous perception and a struggle in making a correct mapping, respectively.

In short, the observations conclude that there are two distinct frequency modes of connectivity, including the low-alpha and low-beta, during the tactile TOJ task. The Low beta mode is essential only when the hands are crossed, and its stronger recruitment leads to superior performance.

Study Funding: This work was supported by KAKENHI (18H0522 and 17H00742) to S.K

General Discussion

I discovered in the first part that the cortical characteristics (thickness and convoluted surface area) in ten anatomical regions, including the right pars-orbitalis, right and left postcentral gyri, left precuneus, left superior parietal lobule, right middle temporal gyrus, left superior temporal gyrus, right cuneus, left supramarginal gyrus, and right rostral middle frontal gyrus was associated with the degree of judgment reversal. The participants with a thinner, larger, and more convoluted cerebral cortex in those ten regions had a superior performance (i.e., a smaller degree of judgment reversal). A larger convoluted surface area is associated with a higher information capacity and a greater specialization (i.e., less interference and a more distinct functionality) (Ringo JL 1991; Tadayon E *et al.* 2020). A thinner cortex corresponds to higher efficiency and proficiency, especially in young adults, the age group of the current study (Schnack HG *et al.* 2015). Therefore, the present findings indicate that a more specialized and efficient functionality of the regions mentioned above led to superior performance. Those functionalities should correspond to correctly mapping tactile stimuli to the hands when the hands are crossed.

Moreover, I found that among those ten regions, the cortical characteristics of the right postcentral gyrus and right pars-orbitalis, together, could most effectively explain the degree of judgment reversal; hence they should be the most critical regions. It has been reported that the postcentral gyrus plays a significant role in integrating the bilateral somatosensory and proprioceptive information (Iwamura Y 1998). It has been found that the pars-orbitalis is associated with top-down inhibitory control (Chavan CF *et al.* 2015; Yoo JH *et al.* 2016). Thus, a more elaborated (efficient) right postcentral gyrus, and right pars-orbitalis should contribute to better integrating tactile spatial representations, and a better inhibitory control on them, respectively.

By studying the brain function during the tactile TOJ task, I discovered in the second part that the brain network mainly functioned in the low alpha band (5~10 Hz) when the hands were uncrossed. However, it operated in the low beta (12~18 Hz) and the alpha band when the hands were crossed. Furthermore, the participants with a smaller degree of judgment reversal more strongly relied on their low beta band connectivity. The beta band is shown to play a significant role in attentional processes and high-level cognitive functions, and its stronger activity was associated with superior performance (Gross J *et al.* 2004; Razumnikova OM 2004; Gola M *et al.* 2013). Therefore, the low beta band connectivity in the crossed posture might correspond to its demand for a high level of alertness and processing power compared to the uncrossed posture. Moreover, a stronger low beta band connectivity might result from a higher level of attention and vigilance, leading to a more robust mapping of the tactile stimuli to the crossed hands (i.e., a superior performance).

Simply put, overall, the present thesis revealed the brain regions that are important in perceiving touch in a crossed-hand posture. Thus, those regions should be associated with the somatosensory and proprioceptive systems and their interactive system. At the structural level, a thinner, larger, and more convoluted cortex contributed to better executing and integrating those systems and, at the functional level, channeling the cortical communications to higher frequencies (low-beta band). The functional and structural properties might be correlated. A thinner, larger, and more convoluted cortex might provide the necessary power for maintaining communications in the low-beta frequency across distance cortical regions. Future studies are needed to reveal this association in detail.

Acknowledgment

First of all, I am thankful to Almighty God who made me able and gave me the opportunity to do this thesis. Without His numerous blessing, it would not have been possible.

I would like to express my deep and sincere gratitude to my supervisor, Professor Shigeru Kitazawa. The completion of this study could not have been possible without his support, meticulous scrutiny, precious comments, and guidance. I am thankful for the many valuable things that he taught me.

Besides my supervisor, I would like to express my appreciation to Dr. Toshimitsu Takahashi. The second part of the thesis could not become reality without using the magnetoencephalography data collected by him. Also, I would like to thank the rest of the professors in the Dynamic Brain Network laboratory, Dr. Tamami Nakano, Dr. Motoaki Uchimura, and Dr. Kei Watanabe, for encouraging me and giving valuable comments on my research.

I want to thank my friends in the laboratory, Chisa Ota, Marina Fukui, and Takuma Hashimoto, for helping me to recruit participants for my study, and Mohammad-Amin Abdollahi, for his encouragement.

Last but not least, I am extremely grateful to my parents for their love, prayers, caring, and sacrifices for educating and preparing me for my future. I dedicate this thesis to my family.

References

Azañón E, Soto-Faraco S. 2008. Changing reference frames during the encoding of tactile events. Current Biology. 18:1044-1049.

Badde S, Heed T. 2016. Towards explaining spatial touch perception: Weighted integration of multiple location codes. Cognitive neuropsychology. 33:26-47.

Badde S, Heed T, Röder B. 2014. Processing load impairs coordinate integration for the localization of touch. Attention, Perception, & Psychophysics. 76:1136-1150.

Badde S, Heed T, Röder B. 2016. Integration of anatomical and external response mappings explains crossing effects in tactile localization: A probabilistic modeling approach. Psychonomic Bulletin & Review. 23:387-404.

Badde S, Röder B, Heed T. 2019. Feeling a Touch to the Hand on the Foot. Current Biology. 29:1491-1497. e1494.

Barnes GR, Hillebrand A. 2003. Statistical flattening of MEG beamformer images. Human brain mapping. 18:1-12.

Belardinelli P, Ortiz E, Barnes G, Noppeney U, Preissl H. 2012. Source reconstruction accuracy of MEG and EEG Bayesian inversion approaches. PloS one. 7:e51985.

Ben-Shabat E, Matyas TA, Pell GS, Brodtmann A, Carey LM. 2015. The right supramarginal gyrus is important for proprioception in healthy and stroke-affected participants: a functional MRI study. Frontiers in neurology. 6:248.

Benjamini Y, Hochberg Y. 1995. Controlling the false discovery rate: a practical and powerful approach to multiple testing. Journal of the Royal statistical society: series B (Methodological). 57:289-300.

Borchers S, Hauser T-K, Himmelbach M. 2011. Bilateral hand representations in human primary proprioceptive areas. Neuropsychologia. 49:3383-3391.

Bullmore E, Sporns O. 2009. Complex brain networks: graph theoretical analysis of structural and functional systems. Nature reviews neuroscience. 10:186.

Cadieux ML, Barnett-Cowan M, Shore DI. 2010. Crossing the hands is more confusing for females than males. Experimental brain research. 204:431-446.

Carpenter B, Gelman A, Hoffman MD, Lee D, Goodrich B, Betancourt M, Brubaker M, Guo J, Li P, Riddell A. 2017. Stan: A probabilistic programming language. Journal of statistical software. 76.

Chavan CF, Mouthon M, Draganski B, Van Der Zwaag W, Spierer L. 2015. Differential patterns of functional and structural plasticity within and between inferior frontal gyri support training‐induced improvements in inhibitory control proficiency. Human brain mapping. 36:2527-2543.

Chen PY, Chen CL, Hsu YC, Cam CAN, Tseng WI. 2020. Fluid intelligence is associated with cortical volume and white matter tract integrity within multiple-demand system across adult lifespan. Neuroimage. 212:116576.

Connolly JD, Andersen RA, Goodale MA. 2003. FMRI evidence for a'parietal reach region'in the human brain. Experimental brain research. 153:140-145.

Crollen V, Lazzouni L, Rezk M, Bellemare A, Lepore F, Collignon O. 2017. Visual experience shapes the neural networks remapping touch into external space. Journal of neuroscience. 37:10097-10103.

Dale AM, Fischl B, Sereno MI. 1999. Cortical surface-based analysis: I. Segmentation and surface reconstruction. Neuroimage. 9:179-194.

De Jong B, Van der Graaf F, Paans A. 2001. Brain activation related to the representations of external space and body scheme in visuomotor control. Neuroimage. 14:1128-1135.

Desikan RS, Ségonne F, Fischl B, Quinn BT, Dickerson BC, Blacker D, Buckner RL, Dale AM, Maguire RP, Hyman BT. 2006. An automated labeling system for subdividing the human cerebral cortex on MRI scans into gyral based regions of interest. Neuroimage. 31:968-980.

Findlater SE, Hawe RL, Semrau JA, Kenzie JM, Amy YY, Scott SH, Dukelow SP. 2018. Lesion locations associated with persistent proprioceptive impairment in the upper limbs after stroke. NeuroImage: Clinical. 20:955-971.

Fischl B. 2012. FreeSurfer. Neuroimage. 62:774-781.

Fischl B, Van Der Kouwe A, Destrieux C, Halgren E, Ségonne F, Salat DH, Busa E, Seidman LJ, Goldstein J, Kennedy D. 2004. Automatically parcellating the human cerebral cortex. Cerebral cortex. 14:11-22.

Friston K, Harrison L, Daunizeau J, Kiebel S, Phillips C, Trujillo-Barreto N, Henson R, Flandin G, Mattout J. 2008. Multiple sparse priors for the M/EEG inverse problem. NeuroImage. 39:1104-1120.

Gola M, Magnuski M, Szumska I, Wróbel A. 2013. EEG beta band activity is related to attention and attentional deficits in the visual performance of elderly subjects. International Journal of Psychophysiology. 89:334-341.

Graziano MS, Cooke DF, Taylor CS. 2000. Coding the location of the arm by sight. Science. 290:1782-1786.

Groh JM, Sparks DL. 1996. Saccades to somatosensory targets. I. Behavioral characteristics. Journal of Neurophysiology. 75:412-427.

Gross J, Schmitz F, Schnitzler I, Kessler K, Shapiro K, Hommel B, Schnitzler A. 2004. Modulation of long-range neural synchrony reflects temporal limitations of visual attention in humans. Proceedings of the national Academy of Sciences. 101:13050-13055.

He B, Astolfi L, Valdés-Sosa PA, Marinazzo D, Palva SO, Bénar C-G, Michel CM, Koenig T. 2019. Electrophysiological brain connectivity: theory and implementation. IEEE Transactions on Biomedical Engineering. 66:2115-2137.

Heed T, Azanon E. 2014. Using time to investigate space: a review of tactile temporal order judgments as a window onto spatial processing in touch. Frontiers in Psychology. 5:76.

Hirsh IJ, Sherrick Jr CE. 1961. Perceived order in different sense modalities. Journal of experimental psychology. 62:423.

Iscan Z, Jin TB, Kendrick A, Szeglin B, Lu H, Trivedi M, Fava M, McGrath PJ, Weissman M, Kurian BT. 2015. Test–retest reliability of FreeSurfer measurements within and between sites: effects of visual approval process. Human brain mapping. 36:3472-3485.

Iwamura Y. 1998. Hierarchical somatosensory processing. Current opinion in neurobiology. 8:522-528.

Karnath H-O, Perenin M-T. 2005. Cortical control of visually guided reaching: evidence from patients with optic ataxia. Cerebral cortex. 15:1561-1569.

Kitazawa S. 2002. Where conscious sensation takes place. Conscious Cogn. 11:475-477.

Kitazawa S, Moizumi S, Okuzumi A, Saito F, Shibuya S, Takahashi T, Wada M, Yamamoto S. 2008. Reversal of subjective temporal order due to sensory and motor integrations. In: Haggard P, Kawato M, Rossetti Y, editors. Attention and Performance XXII, Oxford: Oxford University Press p 73-97.

Linhart H, Zucchini W. 1986. Model selection: John Wiley & Sons.

Lloyd DM, Shore DI, Spence C, Calvert GA. 2003. Multisensory representation of limb position in human premotor cortex. Nature neuroscience. 6:17-18.

López JD, Litvak V, Espinosa JJ, Friston K, Barnes GR. 2014. Algorithmic procedures for Bayesian MEG/EEG source reconstruction in SPM. NeuroImage. 84:476-487.

Lübke J, Feldmeyer D. 2007. Excitatory signal flow and connectivity in a cortical column: focus on barrel cortex. Brain Structure and Function. 212:3-17.

Luders E, Narr KL, Thompson PM, Toga AW. 2009. Neuroanatomical correlates of intelligence. Intelligence. 37:156-163.

Maij F, Seegelke C, Medendorp WP, Heed T. 2020. External location of touch is constructed post-hoc based on limb choice. Elife. 9.

Maris E, Oostenveld R. 2007. Nonparametric statistical testing of EEG-and MEG-data. Journal of neuroscience methods. 164:177-190.

Moharramipour A, Kitazawa S. 2021. What Underlies a Greater Reversal in Tactile Temporal Order Judgment When the Hands Are Crossed? A Structural MRI Study. Cerebral Cortex Communications. 2:tgab025.

Moharramipour A, Mostame P, Hossein-Zadeh G-A, Wheless JW, Babajani-Feremi A. 2018. Comparison of statistical tests in effective connectivity analysis of ECoG data. Journal of neuroscience methods. 308:317-329.

Mostame P, Moharramipour A, Hossein-Zadeh G-A, Babajani-Feremi A. 2019. Statistical Significance Assessment of Phase Synchrony in the Presence of Background Couplings: An ECoG Study. Brain topography.1-15.

Nolte G. 2003. The magnetic lead field theorem in the quasi-static approximation and its use for magnetoencephalography forward calculation in realistic volume conductors. Physics in Medicine & Biology. 48:3637.

Oldfield RC. 1971. The assessment and analysis of handedness: the Edinburgh inventory. Neuropsychologia. 9:97-113.

Ora H, Wada M, Salat D, Kansaku K. 2016. Arm crossing updates brain functional connectivity of the left posterior parietal cortex. Scientific reports. 6:28105.

Overvliet KE, Azañón E, Soto-Faraco S. 2011. Somatosensory saccades reveal the timing of tactile spatial remapping. Neuropsychologia. 49:3046-3052.

Pellijeff A, Bonilha L, Morgan PS, McKenzie K, Jackson SR. 2006. Parietal updating of limb posture: an event-related fMRI study. Neuropsychologia. 44:2685-2690.

Penny WD, Friston KJ, Ashburner JT, Kiebel SJ, Nichols TE. 2011. Statistical parametric mapping: the analysis of functional brain images: Elsevier.

Pienaar R, Fischl B, Caviness V, Makris N, Grant PE. 2008. A methodology for analyzing curvature in the developing brain from preterm to adult. International journal of imaging systems and technology. 18:42-68.

Pöppel E. 1997. A hierarchical model of temporal perception. Trends in cognitive sciences. 1:56-61.

Razumnikova OM. 2004. Gender differences in hemispheric organization during divergent thinking: an EEG investigation in human subjects. Neuroscience Letters. 362:193-195.

Ringo JL. 1991. Neuronal interconnection as a function of brain size. Brain, Behavior and Evolution. 38:1-6.

Röder B, Rösler F, Spence C. 2004. Early vision impairs tactile perception in the blind. Current Biology. 14:121-124.

Ronan L, Pienaar R, Williams G, Bullmore E, Crow TJ, Roberts N, Jones PB, Suckling J, Fletcher PC. 2011. Intrinsic curvature: a marker of millimeter-scale tangential cortico-cortical connectivity? International journal of neural systems. 21:351-366.

Rueda-Delgado LM, Solesio-Jofre E, Mantini D, Dupont P, Daffertshofer A, Swinnen SP. 2017. Coordinative task difficulty and behavioural errors are associated with increased long-range beta band synchronization. NeuroImage. 146:883-893.

Salthouse TA, Habeck C, Razlighi Q, Barulli D, Gazes Y, Stern Y. 2015. Breadth and age-dependency of relations between cortical thickness and cognition. Neurobiol Aging. 36:3020-3028.

Schnack HG, Van Haren NE, Brouwer RM, Evans A, Durston S, Boomsma DI, Kahn RS, Hulshoff Pol HE. 2015. Changes in thickness and surface area of the human cortex and their relationship with intelligence. Cerebral cortex. 25:1608-1617.

Shaw P, Greenstein D, Lerch J, Clasen L, Lenroot R, Gogtay N, Evans A, Rapoport J, Giedd J. 2006. Intellectual ability and cortical development in children and adolescents. Nature. 440:676-679.

Shaw P, Kabani NJ, Lerch JP, Eckstrand K, Lenroot R, Gogtay N, Greenstein D, Clasen L, Evans A, Rapoport JL, Giedd JN, Wise SP. 2008. Neurodevelopmental trajectories of the human cerebral cortex. J Neurosci. 28:3586-3594.

Shibuya S, Takahashi T, Kitazawa S. 2007. Effects of visual stimuli on temporal order judgments of unimanual finger stimuli. Experimental brain research. 179:709-721.

Shore DI, Spry E, Spence C. 2002. Confusing the mind by crossing the hands. Cognitive Brain Research. 14:153-163.

Song C, Schwarzkopf DS, Kanai R, Rees G. 2015. Neural population tuning links visual cortical anatomy to human visual perception. Neuron. 85:641-656.

Soto-Faraco S, Azañón E. 2013. Electrophysiological correlates of tactile remapping. Neuropsychologia. 51:1584-1594.

Sporns O. 2010. Networks of the Brain. MIT press.

Tadayon E, Pascual-Leone A, Santarnecchi E. 2020. Differential contribution of cortical thickness, surface area, and gyrification to fluid and crystallized intelligence. Cerebral Cortex. 30:215-225.

Takahashi T, Kansaku K, Wada M, Shibuya S, Kitazawa S. 2013. Neural correlates of tactile temporal-order judgment in humans: an fMRI study. Cerebral cortex. 23:1952-1964.

Takahashi T, Kitazawa S. 2017. Modulation of Illusory Reversal in Tactile Temporal Order by the Phase of Posterior alpha Rhythm. J Neurosci. 37:5298-5308.

Tian F, Chen Q, Zhu W, Wang Y, Yang W, Zhu X, Tian X, Zhang Q, Cao G, Qiu J. 2018. The association between visual creativity and cortical thickness in healthy adults. Neuroscience letters. 683:104-110.

Unwalla K, Kearney H, Shore DI. 2020. Reliability of the Crossed-Hands Deficit in Tactile Temporal Order Judgements. Multisensory Research. 1:1-35.

Vehtari A, Gelman A, Gabry J. 2017. Practical Bayesian model evaluation using leave-one-out cross-validation and WAIC. Statistics and computing. 27:1413-1432.

Vinck M, Oostenveld R, Van Wingerden M, Battaglia F, Pennartz CM. 2011. An improved index of phase-synchronization for electrophysiological data in the presence of volume-conduction, noise and sample-size bias. Neuroimage. 55:1548-1565.

Wada M, Takano K, Ikegami S, Ora H, Spence C, Kansaku K. 2012. Spatio-temporal updating in the left posterior parietal cortex. PLoS One. 7:e39800.

Wada M, Yamamoto S, Kitazawa S. 2004. Effects of handedness on tactile temporal order judgment. Neuropsychologia. 42:1887-1895.

Wolpert DM, Goodbody SJ, Husain M. 1998. Maintaining internal representations: the role of the human superior parietal lobe. Nature neuroscience. 1:529-533.

Wróbel A, Ghazaryan A, Bekisz M, Bogdan W, Kamiński J. 2007. Two streams of attention-dependent β activity in the striate recipient zone of cat's lateral posterior–pulvinar complex. Journal of Neuroscience. 27:2230-2240.

Yamamoto S, Kitazawa S. 2001. Reversal of subjective temporal order due to arm crossing. Nature neuroscience. 4:759.

Yoo JH, Oh Y, Jang B, Song J, Kim J, Kim S, Lee J, Shin H-Y, Kwon J-Y, Kim Y-H. 2016. The effects of equine-assisted activities and therapy on resting-state brain function in attention-deficit/hyperactivity disorder: a pilot study. Clinical Psychopharmacology and Neuroscience. 14:357.

Publications and Presentations

Publications

Ali Moharramipour, and Shigeru Kitazawa. "What Underlies a Greater Reversal in Tactile Temporal Order Judgment When the Hands Are Crossed? A Structural MRI Study." *Cerebral Cortex Communications*, Vol. 2, No. 2, tgab025, April 2021

Ali Moharramipour, Toshimitsu Takahashi, and Shigeru Kitazawa. " Brain network during tactile temporal order judgment: a MEG connectivity study." *Cerebral Cortex* (***Under preparation***)

Ali Moharramipour. "大脳皮質が薄いほど知能が高くなるというのは本当でしょうか？" *Clinical Neuroscience*, Vol. 39, No. 3, pp. 374-375, March 2021

Posters

Title: Brain network dynamics during a tactile temporal order judgment task: a MEG study

Conference: Japan Neuroscience Society, Kobe, July 2021

Title: What makes you better at tactile temporal order judgment? a structural MRI study

Conference: *Japan Neuroscience Society*, Online, August 2020

Title: What makes you better at tactile temporal order judgment? (Brain regions responsible for making correct tactile temporal order judgment when the hands are crossed)

Conference: *時間生成学 (Chronogenesis),* Osaka, February 2020

Title: Why does arm crossing cause reversal of subjective temporal order? - In search of neural dynamics-

Conference: *FBS Retreat,* Awaji island, May 2019

Title: Brain network dynamics during tactile temporal order judgment: A MEG connectivity study

Conference: *時間生成学 (Chronogenesis),* Matsuyama, February 2019

Talks

Title: What underlies a better tactile temporal resolution and spatial perception?

Location: *Frontier Biosciences colloquium*, December 2020